OBTAINING UNDERWATER ADHESIVE MATERIALS AND CHARACTERIZATION OF THEIR ADHESIVE PROPERTIES TO DIFFERENT SURFACES BY ESR SPECTROSCOPY

A Thesis Submitted to
the Graduate School of Engineering and Sciences of
İzmir Institute of Technology
in Partial Fulfillment of the Requirements for the Degree of

MASTER OF SCIENCE

in Material Science and Engineering

by
İklima KIRPAT

July 2016
İZMİR

We approve the thesis of **İklima KIRPAT**

Examining Committee Members:

Asst. Prof. Dr. Yaşar AKDOĞAN
Department of Materials Science and Engineering, İzmir Institute of Technology

Asst. Prof. Dr. Ufuk ŞENTÜRK
Department of Materials Science and Engineering**,** İzmir Institute of Technology

Asst. Prof. Dr. Nesrin HORZUM POLAT
Department of Engineering Sciences, İzmir Katip Çelebi University

22 July 2016

Asst. Prof. Dr. Yaşar AKDOĞAN
Supervisor, Department of Materials Science and Engineering,
İzmir Institute of Technology

Prof. Dr. Mustafa Muammer DEMİR
Head of the Department of Material Science and Engineering

Prof. Dr. Bilge KARAÇALI
Dean of the Graduate School of Engineering and Science

ACKNOWLEDGEMENTS

There are a number of people who have assisted me during my graduate education. First of all, I would like to thank my supervisor, Asst. Prof. Dr. Yaşar AKDOĞAN for his patience, encouragement and excellent guidance on the research which I performed. It was a pleasure for me to work in the field of underwater adhesive materials, and it was honour to study with him.

I would like to thank Ceyla ÇETİNTAŞ, Muhammed ÜÇÜNCÜ, Pınar DEVECEL, Erman KARAKUŞ, Hüseyin ZEYBEK, Duygu TATLIDİL, and Anıl ÖZDEMİR.

My special thanks to Assoc. Dr. Mustafa EMRULLAHOĞLU for permission to enable using his laboratory facilities and his support on my thesis.

Also I would like to thank Asst. Prof. Dr. Nesrin HORZUM POLAT and Asst. Prof. Dr. Ufuk ŞENTÜRK for participating as a committee member and reviewing my work.

I would like to thank the TUBİTAK (114Z318) and IZTECH for supporting me during this project.

Endless gratitude is also extended to my parents, İbrahim KIRPAT and Hamdiye KIRPAT, my brother, Kerim KIRPAT and sister, Tuğba KIRPAT and all my friends for providing love and support every time that I got desperate. I love them very much.

ABSTRACT

OBTAINING UNDERWATER ADHESIVE MATERIALS AND CHARACTERIZATION OF THEIR ADHESIVE PROPERTIES TO DIFFERENT SURFACES BY ESR SPECTROSCOPY

This study describes the design, synthesis and spectral behavior of underwater adhesive materials which adhere to surfaces without any external force.

The materials with wet adhesive properties have a wide application field from biomedical implantation and covering to antifouling materials. Mussel's stickiness to rocks, ships, etc. inspite of strong waves in the sea inspires us to synthesize adhesives materials. Mussels attach to solid surfaces strongly using their threads and plaques. The complex fluid (mussel foot proteins, Mfps) secreted from mussels is solidified in the sea water and forms threads, each equipped with a distal adhesive plaque. Mfps have large amount of L-3,4-dihydroxyphenylalanine (DOPA) amino acid and this amino acid is responsible for adhesion of mussels to underwater surfaces. The presence of stable hydration layers around both the adhesive materials and surface results in strong hydration repulsive forces that undermine adhesion. So far, applied external forces were used to break through or disrupt the hydration layers which prevent adhesion.

In this research branched PEG based polymers were modified with different amounts of DOPA in order to obtain underwater adhesive material. Their adhesive properties to spin labeled (SL) nanoparticles were tested without applying an external force by electron spin resonance (ESR) spectroscopy. As model surfaces we synthesized hydrophobic SL-polystyrene and hydrophilic SL-silica nanoparticles. ESR results showed that four arm DOPA modified PEG is able to adhere to SL-polystyrene but not to SL-silica. Moreover, adhesions of the polymers were tested by making hydrogels using iodate (IO_3^-) and iron (III) (Fe^{3+}) ions. ESR results showed that hydrogels prepared from four arm DOPA modified PEG/IO_3^- mixture has better adhesive property to SL-polystyrene compare to hydrogels prepared from four arm DOPA modified PEG/Fe^{3+} mixture and adhesion of IO_3^- based gel form is better compared to molecule form.

.

ÖZET

SULU ORTAMDA YAPIŞKANLIK ÖZELLİĞİ GÖSTEREBİLEN MALZEMELERİN ELDE EDİLMESİ VE FARKLI YÜZEYLERE OLAN YAPIŞKANLIKLARININ ESR SPEKTROSKOPİSİ İLE ÇALIŞILMASI

Bu çalışmada su altında kuvvet uygulamadan yapışabilen malzemeler sentezlenmiş ve yüzeylere olan yapışkanlıkları ESR spektroskopisi ile gözlemlenmiştir.

Su içerisinde yapışkanlık özelliği gösterebilen malzemeler, biyomedikal implantasyon ve kaplamalardan gemilerde çürümeyi önleyecek materyallere kadar geniş bir uygulama alanına sahiptir. Midyelerin denizin içerisinde tutundukları yüzeylerden güçlü dalgalara rağmen kopmamaları ıslak ortamda yapışabilen malzemelerin üretilebileceğini göstermektedir. Midyelerin salgıladıkları kompleks salgıların (mussel foot protein, Mfp) deniz suyunun içerisinde katılaşması sonucunda oluşan iplikler ile bu ipliklerin ucunda oluşan plaklar midyelerin yüzeylere güçlü bir şekilde yapışmasını sağlamaktadır. Mfp'ler üzerinde yapılan çalışmalar midyelerin büyük oranda DOPA amino asidini içerdiğini ve DOPA'nın yapışma üzerinde büyük bir etkisinin olduğunu göstermiştir. Su içerisinde, yapışkan malzemenin ve yapışılacak yüzeyin çevrelerinde oluşan kuvvetli hidrasyon katmanları tutunmayı engelleyen önemli bir etkendir. Şimdiye kadar olan çalışmalarda, dışarıdan kuvvet uygulayarak yapışmayı engelleyen hidrasyon katmanları zayıflatılmıştır.

Bu tez çalışmasında 4 kollu PEG polimeri üzerine farklı miktarlarda DOPA amino asidi eklenerek hiçbir kuvvet uygulamadan su altında spin etiketli nanoparçacık yüzeylerine yapışabilecek malzeme elde edilmiştir. Elde edilen malzemelerin yapışkanlıkları electron spin resonans (ESR) spektroskopisi ile test edilmiştir. Model yüzey olarak spin etiketli hidrofobik polistiren ve hidrofilik silika nano parçacıkları kullanılmıştır. Yapışkanlığı arttırabilmek için IO_3^- ve Fe^{3+} iyonları kullanılarak jel haline getirilmiştir. Yapılan ESR ölçümlerinde dört kolunda DOPA olan polietilen glikol maddesinin spin etiketli polistiren nanoparçacığı üzerine yapıştığı fakat spin etiketli silica nanoparçacığı üzerine yapışmadığı gözlemlenmiştir. Ayrıca yapılan ESR ölçümlerine göre IO_3^- iyonu ve PEG-$(DOPA)_4$ ile elde edilen jelin yapışkanlığının Fe^{3+} iyonu ve PEG-$(DOPA)_4$ ile elde edilen jele göre daha iyi olduğu gözlemlenmiştir. Ayrıca IO_3^- iyonu ile elde edilen jelin, jel olmayan maddeye göre daha iyi yapıştığı gözlemlenmiştir.

TABLE OF CONTENTS

LIST OF FIGURES

Figure **Page**

LIST OF TABLE

Table **Page**

LIST OF ABBREVIATIONS

DOPA	L-3,4-dihydroxyphenylalanine
Mfps	Mussel Foot Proteins
TFA	Trifluoroacetic Acid
Trp	Tryptophane
THF	Tetrahydrofuran
DCM	Dichloromethane
DMSO	Dimethyl Sulfoxide
SLPS	Spin Labeled Polystyrene Nanoparticle
SLSi	Spin Labeled Silica Nanoparticle
Et_3N	Triethylamine
MES	2-(*N*-morpholino)ethanesulfonic acid
PEG	Polyethylene glycol
ESR	Electron Spin Resonance
NMR	Nuclear Magnetic Resonance
UV-Vis	Ultraviolet-visible

CHAPTER 1

INTRODUCTION

1.1. Mussel Foot Proteins (Mfps)

Mussels have an ability to adhere to marine surfaces. They secrete protein adhesives to attach to the substrates where they reside. Mussels secret the liquid protein adhesives in order to form a solid adhesive plaque which can attach to very different wet surfaces, such as wood structures, metal, rocks and polymer ship hulls (Dalsin et al., 2003). They attach to these kinds of surfaces by their byssus in the sea (Figure 1.1).

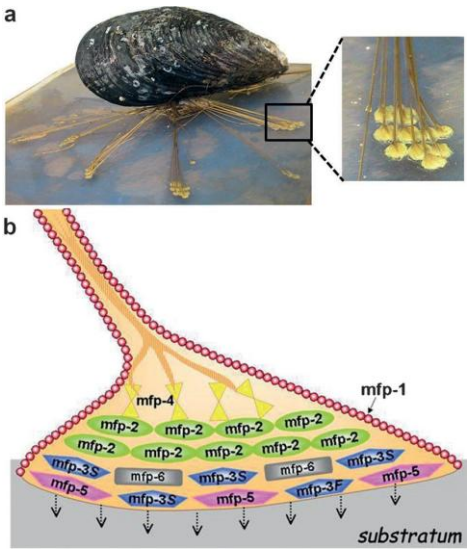

Figure 1.1. **(**a) A mussel (Mytilus californianus) attached to the surface of substratum by a byssus essentially a bunch of adhesive-tipped threads. (b) Schematic representation of one of the adhesive tips or plaques in (a) enlarged to show the approximate location of known Mfps (Source: Akdogan et al., 2014).

Byssus have aproximately 25–30 different proteins and 7–8 of these may present in the plaque, but only 5 of them unique to plaque which collectively determine the adhesive properties of the plaque (Lee et al., 2011). The proteins that confined to plaques are Mfp-1, Mfp-2, Mfp-3, Mfp-4, Mfp-5, and Mfp-6 and pre-Cols (Lee et al., 2011). One of the unique features of Mfps is the presence of L-3,4-dihydroxyphenylalanine (DOPA) which is an amino acid that is believed to be responsible for both crosslinking and adhesion characteristics of Mfps (Table 1.1). The catechol form of DOPA is believed to be responsible for adhesion to substrates (Zeng et al., 2000).

Protein	Mass, kDa	pI	DOPA, mol%	Location
mfp-1	108	10	10–15	Cuticle
mfp-2	45	9	5	Plaque
mfp-3	5–7	8–10	10–20	Plaque
mfp-4	90	10.5	2	Plaque
mfp-5	9	9–10	30	Plaque
mfp-6	11	10	2	Plaque
preColD	240	9	<1	Thread, plaque
preColNG	240	9	<1	Thread, plaque

Table 1.1. Comparison of the DOPA content of proteins in the threads of *Mytilus* species and adhesive plaques (Source: Lin et al., 2006)

1.2. DOPA (3,4-dihydroxyphenylalanine) and Cross Linking

DOPA is formed by posttranslational modification of tyrosine (Figure 1.2).

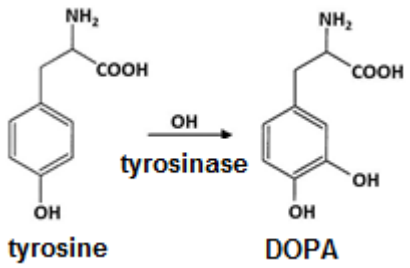

Figure 1.2. Formation of DOPA molecule from tyrosine

When DOPA is oxidized to o-quinone, crosslinking can be observed. So the catechol form of DOPA is thought to be responsible for adhesion to any surface. However, DOPA and metal ions complexation could contribute to bulk crosslinking adhesion in the meantime. For instance, Fe^{3+} forms excessively stable coordination complexes with various catechols (Zeng et al., 2000). Binding of one, two, or three DOPAs to each metal nucleus is affected by the ratio of Fe^{3+} to DOPA. Crosslinking of proteins occurs at least when two DOPA molecules come together (Figure 1.3).

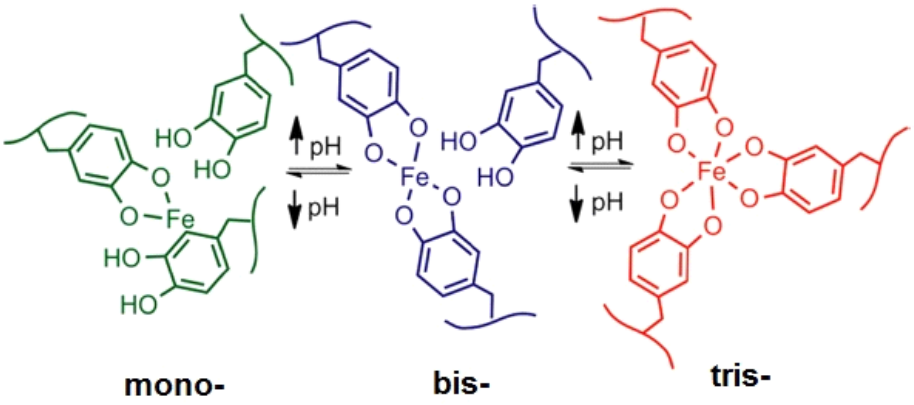

Figure 1.3. The cross-linking mechanism of catechol groups by Fe^{3+} ion with increasing pH (Source: Krogsgaard et al., 2013)

The certain mechanism of the interaction of adhesive proteins and surfaces has not been completely revealed. DOPA has been found as essential for mussel adhesion as a result of its cross-linking ability (Figure 1.4). The predicted DOPA cross-linking mechanisms involve enzymatic oxidation, disulfide formation, chemical oxidation, and metal chelation (Leng et al., 2013).

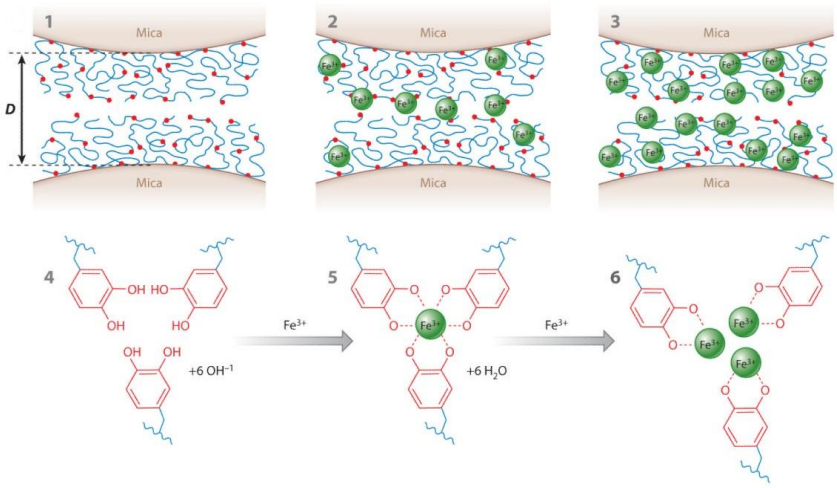

Figure 1.4. Fe^{3+} bridging of Mfp-1 films on mica surface (*1*) without Fe^{3+}, (*2*) with 10-µM Fe^{3+}, and (*3*) with 100-µM Fe^{3+}. Also the chemical interactions between DOPA and Fe^{3+} are shown: (*4*) no Fe^{3+}, (*5*) tris-DOPA-Fe^{3+} complexes, and (*6*) mono-DOPA-Fe^{3+} complexes. (Source: Lee et al.,2011)

1.3.DOPA Modified Polymers

Due to magnificent adhesive performance of mussel foot proteins in wet and turbulent environments, they represent attractive targets for biomimetic purposes. Biomimetic structures offer the chance to have native proteins' functional properties in synthetic systems. Since DOPA has been accepted as being a main component of many mussel foot proteins, with both adhesive and cohesive roles, linear or branched polymers have been frequently functionalized with DOPA. This approach can be made by a family of poly(ethylene glycol) (PEG) which is based linear and branched polymers and here DOPA is combined as a terminal group on each polymer chain (Figure 1.5) (Lee et al., 2011).

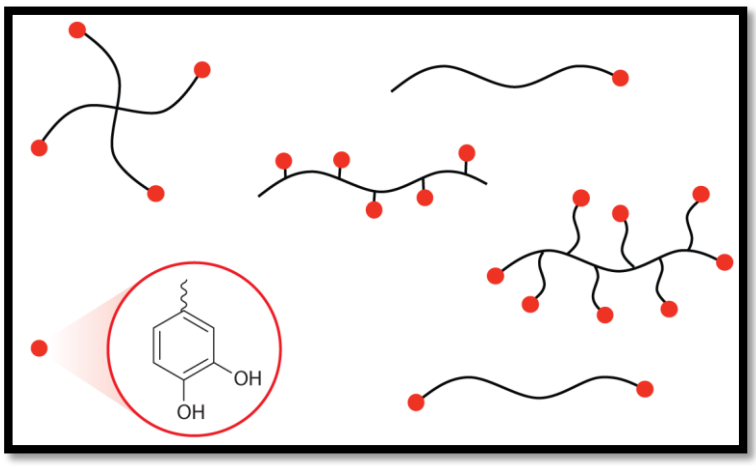

Figure 1.5. Schematic illustration of mimetic polymer systems of mussel adhesive protein. The red circles shows DOPA or a catechol mimic of DOPA which covalently bonded to polymer chain ends or as side chains of polymerizable catechol monomers. (Lee et al., 2011)

1.4. Adhesion Measurements of DOPA to Different Wet Surfaces

The adhesion properties to different surfaces of DOPA modified polymers were measured by X-ray photoelectron spectroscopy (XPS) (Dalsin et al., 2002), sum frequency generation (SFG) spectroscopy (Leng et al., 2013), atomic force microscopy (AFM) (Lee et al., 2006), surface force apparatus (SFA) (Yu et al., 2011) and lap shear techniques (Matos-Perez et al., 2012). Figure 1.6 shows some of these techniques, e.g. AFM, SFA, and lap shear technique. In these techniques the polymers were adhered to chosen surfaces by applying external forces and after that the separation forces of adhered surfaces were determined.

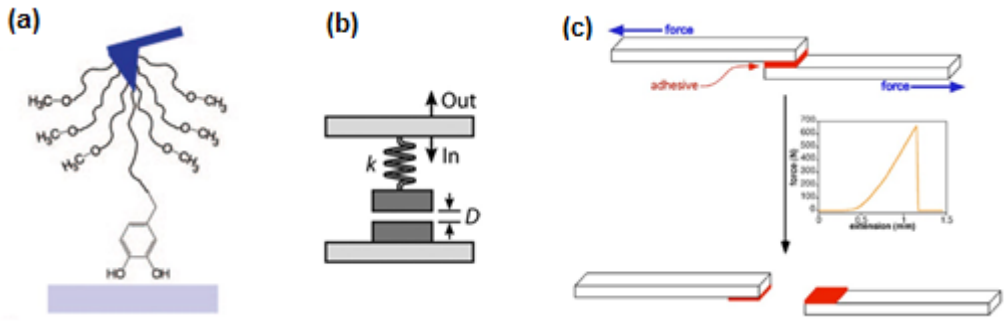

Figure 1.6. The techniques which are used in the literature to measure adhesion properties of synthetic DOPA modified polymers. These techniques were applied in aqueous medium, and external forces were applied to these polymers for the adhesion (a) Atomic force microscope, (AFM) (Source: Lee et al., 2006). (b) Surface force apparatus (SFA). (Source: Yu et al., 2011). (c) Lap shear technique (Source: Matos-Perez et al., 2012).

Sum frequency generation spectroscopy (SFG) and X- ray photoelectron spectroscopy were used to determine the polymers which are adhered to surfaces. It is also possible to observe the adhesion interactions between surface of nanoparticles and Mfps by ESR spectroscopy (Akdogan et al., 2014).

1.5. Electron Spin Resonance (ESR) Spectroscopy

ESR spectroscopy is a technique which is used to measure the paramagnetic properties of samples. If samples do not have any paramagnetic property, samples can be transformed into ESR active by using spin label technique. Stable nitroxide radicals can be used for this purpose.

Every electron has a spin quantum number and magnetic moment with magnetic components (m_s=1/2) and (m_s=-1/2). In the presence of an external magnetic field (B), the electron's spin magnetic moment (μ) aligns itself either parallel (-1/2) or antiparallel (+1/2) to the field, each of them have a specific energy (E).

$$E = \mu B \tag{1.1}$$

The spin magnetic moment (μ) of free electron is given by;

$$\mu = (-1/2)g_e\beta \tag{1.2}$$

where g_e is the free electron Zeeman (correction) factor and β is the Bohr magneton. g-factor is a signature for a material and it has the value of 2.0023 for the free electron. Bohr magneton equals to 9.2700949 x 10^{-24} JT^{-1}.

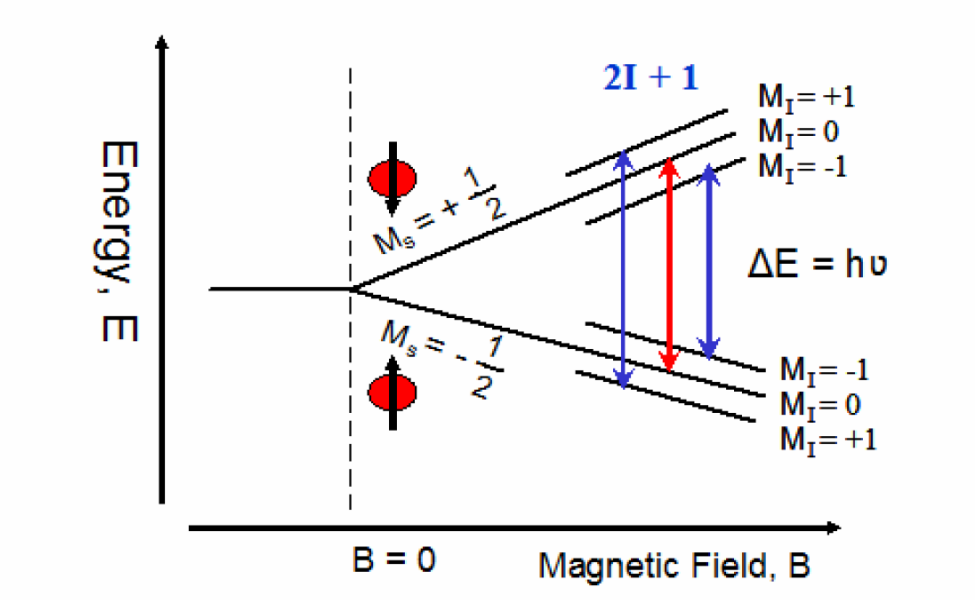

Figure 1.7. Principle of ESR spectroscopy, energy vs magnetic field diagram. (Akdogan Ph.D. thesis, 2009)

At a constant microwave frequency, energy levels of electron spin states separate when the magnetic field is applied. The lower and higher energy states occur. At the resonance condition the difference between two electon spin states (E_α = +1/2 $g_e\beta B$ and E_β =-1/2 $g_e\beta B$) equals to the microwave energy:

$$\Delta E = h\upsilon = g_e \beta_e B \tag{1.3}$$

where υ is the microwave frequency and h is the Planck's constant.

In an ESR spectrum, the signal of an electron is split by neighboring nuclei and this is called hyperfine interaction. Interaction of the electron spin with a nuclear spin (I≠0) causes additional splittings (Figure 1.7).

$$\text{number of splittings} = 2nI+1 \qquad (1.4)$$

In order to calculate number of splittings the above equation is used. Here 'n' is the number of equivalent nuclei around electron and 'I' is the nuclear spin number. For instance the nitroxide radical (NO·) has three equivalent signals in ESR spectrum, because the nuclear spin number of oxygen (O) is zero and nuclear spin number for nitrogen is one and the number of effective nuclei nitrogen (N) around radical is one so,

$$\text{number of splitting } (NO\cdot) = 2(1)(1)+1 = 3$$

Dynamic properties of spin labels can be analyzed from the shape of ESR signals (Jeschke et al., 2008). If the duration of rotational correlation time of spin label is short, the spectrum has sharp signals. On the other hand, if the duration of rotational correlation time of spin label is long, the spectrum has broad signals (Figure 1.8). The radical in nonviscous solution has 3 equivalent signals due to its isotropic motions with same rotational speeds in three directions, but when it is in medium which affects its rotational motion, the signals are not any more equal to each other because of its anisotropic motion. For radicals which have anisotropic motion, the rotational speeds in three directions are not equal and the rotational motion generally slows down (Figure 1.8).

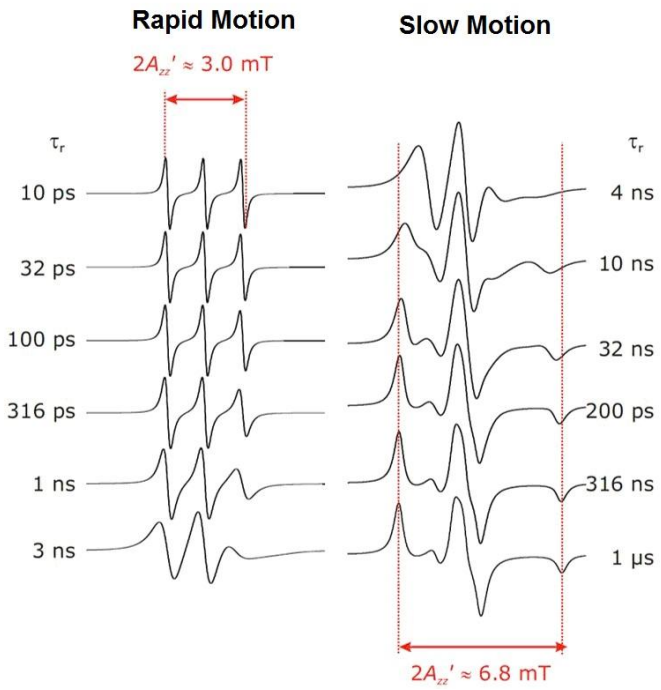

Figure 1.8. ESR spectra of stable nitroxide radical when it has fast and slow motions in aqueous medium (Source: Jeschke et al., 2008)

Common spin labels used in the literature are 2,2,6,6-Tetramethylpiperidin-1-yl)oxyl (TEMPO) based radicals. Different TEMPO based radicals with different functional groups are commercially available. Four methyl groups around the nitroxide radical protect the radical and keep it stable. Functional groups (Figure 1.9) on the spin label can make covalent bonds with functional groups on the nanoparticle surfaces.

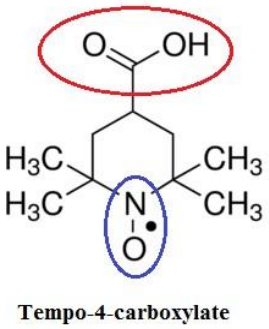

Figure 1.9. Functional group of Tempo-4-carboxylate (red circle), radical group of Tempo-4- carboxylate (blue circle)

It is also possible to find out the states of spin label, free or bound to nanoparticle, using ESR spectroscopy. In solution free (unbound) labels have sharp signals because of freely rotational motion. On the other hand, bound spin labels have broad signals due to their restricted motion. (Figure 1.8).

1.6. Some Literature Studies of DOPA Adhesion

Lately, underwater adhesive materials have attracted great attention and plenty of studies were reported (Lee et al., 2011). Mussel foot proteins are an option to study properties of underwater adhesive materials. For this purpose Akdogan et. al worked on different mussel foot proteins and they showed that Mfp-3s can adhere to surface of polystyrene nanoparticles without applying of any force. They used ESR spectroscopy and Dynamic Nuclear Polarization technique to measure the adhesion of Mfps. ESR spectra of SLPS before and after the addition of Mfps show different rotational correlation times (Figure 1.10). For example the found correlation time of SLPS is 4.2 ns and after addition of Mfp-3S the correlation time increases and it becomes 5.7 ns. This shows that Mfp-3S binds to SLPS and restrict the motion of spin label (SL) on polystyrene (PS). Figure 1.10 shows the spectrum of free SL in buffer. Its rotational correlation time is 20 ps.

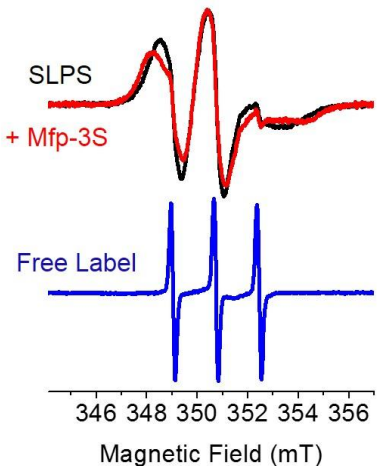

Figure 1.10. ESR spectra of SLPS before (black) and after addition of Mfp-3S (slow; red) in 2-(N-morpholino)ethanesulfonic acid (MES) buffer (pH 3.0) at 20 °C, and ESR spectrum of free 4-carboxy-2,2,6,6- tetramethylpiperidin-1-oxyl, in MES buffer at pH 3.0 (blue) (Source: Akdogan et al., 2014)

As it was mentioned before, DOPA is the key molecule to adhere to surfaces and so Lee and his group measured the single molecule adhesion force of DOPA by AFM in 2006 (Lee et al., 2006). They revealed a high strength yet fully reversible noncovalent interaction between DOPA and wet metal oxide surface (Figure 1.11). According to that study DOPA uses a combination of chemical multi-functionality and high strength to adhere to substrates of very different composition from organic to metallic.

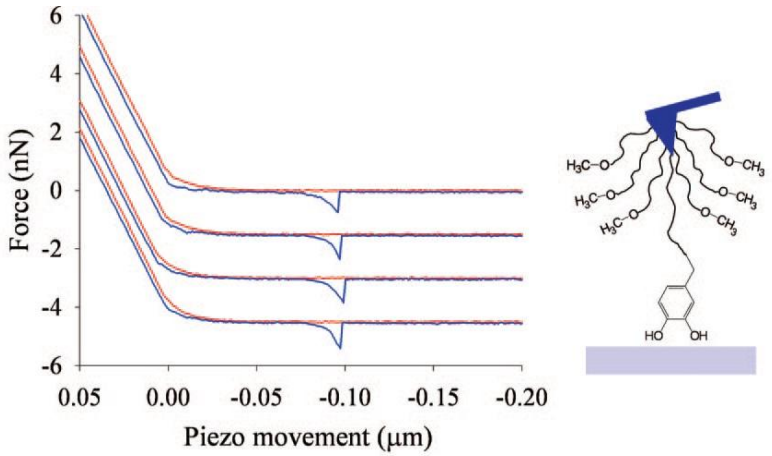

Figure 1.11. DOPA adheres reversibly and strongly to Ti surfaces. Schematic of DOPA-functionalized AFM tip and single-molecule F–D curves of DOPA interacting with surface of Ti. (Source: Lee et al., 2006)

Obtaining large quantities of the biological materials that contain DOPA is a difficult work. Westwood et al. showed synthesis, reactivity and adhesive characteristics of polymers which mimic bioadhesives (Westwood et.al., 2007). They used a polystyrene backbone to take the place of Mfp's polyamide chain. Also cross-linkable catechol groups were used and they were appended to the polystyrene. They used different cross-linker groups and tested the adhesive property of synthesized polymers which contain different amounts of 3,4-dihydroxystyrene. They used the lap shear technique. Their results showed that poly[(3,4-dihydroxystyrene)-*co*-styrene] has an adhesive strength of 1.2 MPa and this value is very close to adhesive strength of mussel foot protein poly-lysine-DOPA (1.5 MPa).

The materials with wet adhesive properties have a wide application field from biomedical implantation and covering to antifouling materials for ships. Mussel's

stickiness to surfaces inspite of strong waves in the sea inspires us to synthesize adhesives mimicking mussel's adhesive proteins that adhere well in wet environment. As an alternative method to X-ray photoelectron spectroscopy (XPS) (Dalsin et al., 2002), sum frequency generation (SFG) spectroscopy (Leng et al., 2013), atomic force microscopy (AFM) (Lee et al., 2006), surface force apparatus (SFA) (Yu et al., 2011) and lap shear techniques (Matos-Perez et al., 2012) we used ESR spectroscopy to measure the adhesive property of synthesized adhesives mimicking mussel's adhesive proteins. The other important thing here is the synthesized sample adhered to the model surface by itself underwater. We did not apply any external force.

CHAPTER 2

EXPERIMENTAL STUDY

2.1. General Methods

All reagents were purchased from commercial suppliers (Aldrich and Merck) and used without further purification. ^{1}H NMR was measured on a Varian VNMRJ 400 Nuclear Magnetic Resonance Spectrometer. 5 mg of synthesized polymers were dissolved in 0.5 ml of deuterated NMR solvents. UV absorption spectra were obtained on Shimadzu UV-2550 Spectrophotometer. Samples were placed in quartz cuvettes with a path length of 10.0 mm (2.0 mL volume). pH was recorded by HI-8014 instrument (HANNA). All measurements were conducted at least in triplicate. ESR was measured on Adani CMS 8400 ESR Spectrometer. The synthesized polymers were dissolved in 2-(*N*-morpholino) ethanesulfonic acid (MES) buffer. 6 µl of spin labeled polystyrene was mixed with 3 µl of synthesized polymer (90 mg / 1 ml) and 7 µl of the mixture was put into quartz ESR tube.

2.2. Synthesis Section

2.2.1. Synthesis of N-Boc-L-DOPA

In an ice bath (0 ^{o}C), L-DOPA (78.85 mg, 0.4 mmol) and triethylamine (86 µL) were mixed in Dichloromethane (DCM):Dioxane (1:1) mixture (800 µL). The mixture was stirred at 0 ^{o}C until all compunds were dissolved. Afterwards, di-tert-butyl dicarbonate (98mg, 0.45 mmol) was dissolved in dioxane (400 µL) and added into the first mixture and stirred at 0 ^{o}C for 30 min. After 30 min the mixture was stirred at 25 ^{o}C for 17 hours. At the end of the reaction, the mixture was extracted with ethyl acetate (50 ml) and the pH of the organic phase was adjusted to 1 by HCl (1N) and back extracted with ethyl acetate (50 ml) for 3 times. Combined organic phases were dried over Na_2SO_4. Organic solvent was evaporated to afford N-Boc-L-DOPA (Figure 2.1) as a brown oil

which was used in the next step without any purification. (100.4 mg, 80% yield) (Giorgioni et al., 2010). In the NMR spectrum of this molecule (Figure A.1, appendix) the integration of amide proton, which is one, was taken as reference and so at 1.30 ppm we observed the 9 protons of protected group, this showed that protected group made bond with DOPA. So NMR result proved that the molecule was synthesized. Proton NMR signals of molecule were observed at following ppm values; ^{1}H NMR (400 MHz, DMSO-d_6) δ: 6.87 (d, 1H), 6.58 (d, 2H), 6.44 (d, 1H), 4.01-3.93 (m, 1H), 2.79-2.58 (m, 2H), 1.30 (s, 9H)

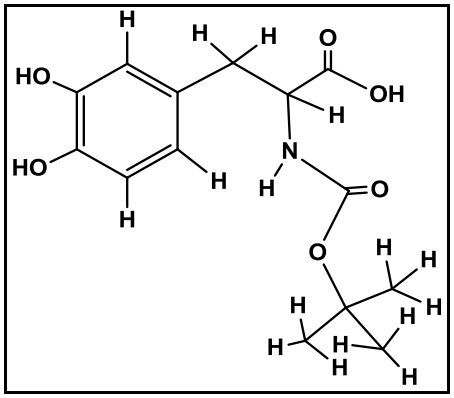

Figure 2.1. Molecular structure of N-Boc-L-DOPA

2.2.2. Synthesis of PEG-(N-Boc-L-DOPA)$_4$

PEG-$(NH_2)_4$ (10,000 g/mol) (97 mg, 9.7x10^{-3} mmol), N-Boc-L-DOPA (23.9 mg, 80 mmol), 1-hydroxybenzotriazol (HOBT) (17.3 mg, 0.128 mmol), and triethyl amine (17.6 µL) were mixed in a mixture of DCM (460 µL) and DMF (460 µL) at 25 ^{o}C until all compunds dissolved. After that 2-(1H-benzotriazol-1-yl)-1,1,3,3-tetramethyluronium hexafluorophosphate (HBTU) (29.6 mg, 0.078 mmol) and DCM (460 µL) were added into the mixture and it was stirred at 25 ^{o}C under argon atmosphere for 5 hours. At the end of the experiment ninhydrin test was applied to control whether there is any primary amine in the experiment medium. 2-3 drops of product was dissolved in DCM (1 ml) and 2-3 drops of ninhydrin solutuion was put into this mixture. The mixture was stirred at 50 ^{o}C for 30 min, the test result was negative (Figure 2.2, b). The crude product was washed with saturated sodium chloride solution (50 ml), $NaHCO_3$ (5% w/ml) solution, HCl (1 M) solution (50 ml), and distilled water (50 ml). The organic phase was dried over Na_2SO_4 and the product was precipitated in cold diethyl ether for 3 times to afford PEG-(N-Boc-

L-DOPA)$_4$ (Figure 2.2, b) as brown solid (75.5 mg, 70% yield) (Lee et al., 2002). In the NMR spectrum of this molecule (Figure A.2, appendix) the integration of methylene protons of polyethylene glycol (896H) was taken as reference and 36 protons at 1.41 ppm showed that N-Boc-L-DOPA made bond with four arm of PEG. Proton NMR signals of molecule were observed at following ppm values; ^{1}H NMR (400 MHz, $CDCl_3$) δ: 6.76 (t, 8H), 6.57 (d, 4H), 6.14 (s, 4H), 4.20 (s, 4H), 3.79 (t, 8H), 3.62-3.39 (m, 896H), 3.02 (d, 8H), 2.72 (t, 8H), 1.41 (s, 36H).

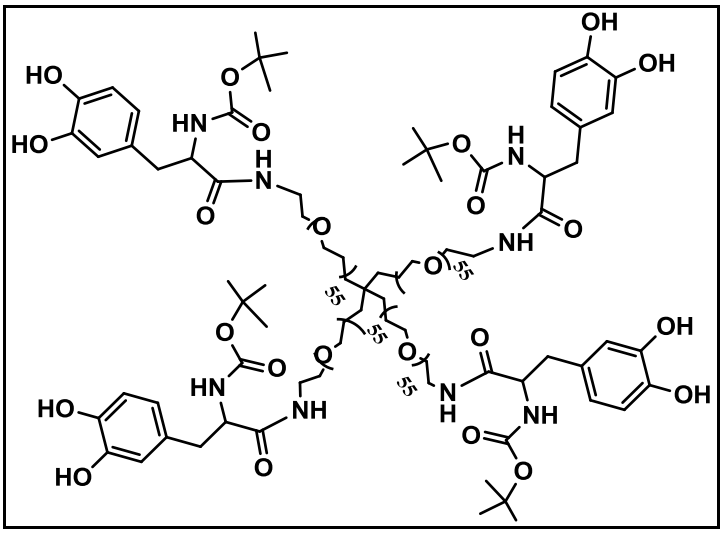

Figure 2.2. Molecular structure of PEG-(N-Boc-L-DOPA)$_4$

Figure 2.3. a) Positive primary amine test result of PEG-$(NH_2)_4$, b) Negative primary amine test result of PEG-(N-Boc-L-DOPA)$_4$

2.2.3. Synthesis of PEG-(DOPA)$_4$

In an ice bath (0 ^oC), L-DOPA PEG-(N-Boc-L-DOPA)$_4$ (75.5 mg, 6.78x10^{-3} mmol) was dissolved in DCM (2 ml), and three fluoroacetic acid (TFA) (406 µL) was added. The mixture was stirred at 25 ^oC for an hour. After evaporating the solvent the crude product was precipitated in cold diethyl ether for 3 times to afford PEG-(DOPA)$_4$ (Figure 2.4) as light green solid (58 mg, 80% yield) (Lee at al., 2002). After purification step the NMR spectrum (Figure A.3, appendix) showed that the signal of 36 protons at 1.41 ppm dissappeared. So it proved that the protected group removed from the molecule. Proton NMR signals of molecule were observed at following ppm values; ^{1}H NMR (400 MHz, $CDCl_3$) δ: 6.76 (t, 8H), 6.57 (d, 4H), 6.14 (s, 4H), 4.20 (s, 4H), 3.79 (t, 8H), 3.62-3.39 (m, 896H), 3.02 (d, 8H), 2.72 (t, 8H).

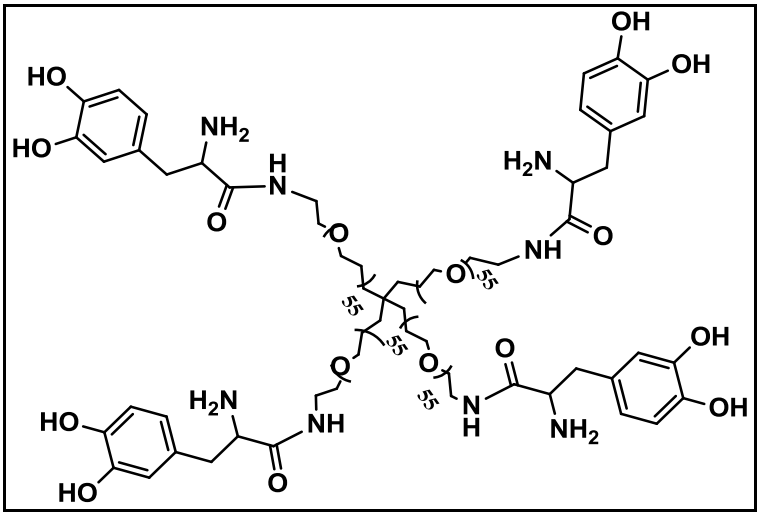

Figure 2.4. Molecular structure of PEG-(DOPA)$_4$

2.2.4. Synthesis of PEG-(p-nitrophenyl carbonate)$_4$

PEG-(OH)$_4$ (10,000 g/mol) (214 mg, 21.4x10^{-3} mmol) and p-nitrophenyl chloroformate (51.4 mg, 255x10^{-3} mmol) were mixed in dry DCM (3.5 ml), and stirred for 15 min under argon atmosphere. Afterwards, dry triethyl amine (25 µL) was added and the mixture was stirred at 25^{o}C for 24 hours. At the end of the experiment TFA was added into the experiment until the color of the experiment turned to colorless from yellow. After that the solvent was evaporated at rotary and the crude product precipitated

in cold diethyl ether for 3 times to afford PEG-(p-nitrophenyl carbonate)$_4$ (Figure 2.5) as white powder (161 mg, 71% yield) (Mueller et al., 2011). In the NMR spectrum of this molecule (Figure A.3, appendix) the integration of methylene protons of polyethylene glycol (896H) was taken as reference and 8 protons signal at 8.30 and 7.55 ppm, which belong to p-nitrophenyl chloroformate, showed that p-nitrophenyl chloroformate made bond with four arm of PEG. Proton NMR signals of molecule were observed at following ppm values; ^{1}H NMR (400 MHz, DMSO-d$_6$) δ: 8.30 (d, 8H), 7.55 (d, 8H), 4.35 (t, 8H), 3.69 (t, 8H), 3.49 (s, 896H).

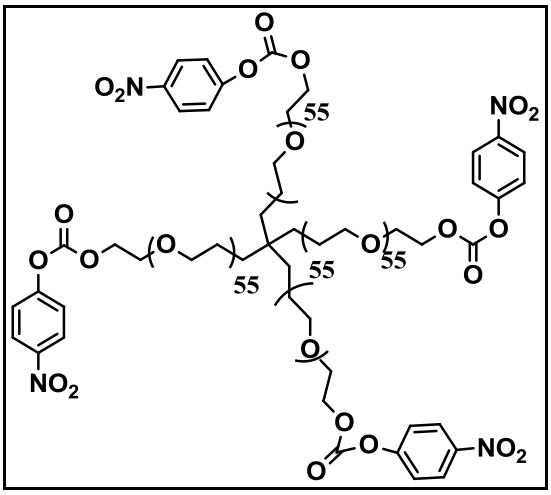

Figure 2.5. Molecular structure of PEG-(p-nitrophenyl carbonate)$_4$

2.2.5. Synthesis of PEG-(Trp)$_4$

Tryptophane (122 mg, 0.6 mmol) and PEG-(p-nitrophenyl carbonate)$_4$ (161 mg, 15x10^{-3} mmol) were mixed in dry DMSO (3 ml). The mixture was stirred at 25 ^{o}C for 5 hours. Next the experiment was cooled to 0 ^{o}C and the pH of the experiment was adjusted to 3 by using HCl (2 M) solution. After that the crude product was extracted with distilled water for 8 times and dried over Na_2SO_4. Next, solvent was evaporated at rotary and the crude product precipitated in cold diethyl ether for 3 times to afford PEG-(Trp)$_4$ (Figure 2.6) as white powder (81 mg, 50% yield) (Mueller at al., 2011). In the NMR spectrum of this molecule (Figure A.4, appendix) the integration of methylene protons of polyethylene glycol (896H) was taken as reference and 8 protons signal at 8.30 and 7.55 ppm, which belongs to p-nitrophenyl chloroformate were disappeared and at 10.75 ppm the signal of 4 protons of tryptohans were observed. Also the other proton signal of tryptophan

molecule were observed with excepted integral values. Proton NMR signals of molecule were observed at following ppm values; ^{1}H NMR (400 MHz, DMSO-d_6) δ: 10.75 (s, 4H), 7.49 (d, 4H), 7.30 (d, 4H), 7.11 (s, 4H), 7.03 (t, 4H), 6.94 (t, 4H), 4.14-4.09 (m, 8H), 3.48 (m, 896H), 3.13 (d, 8H).

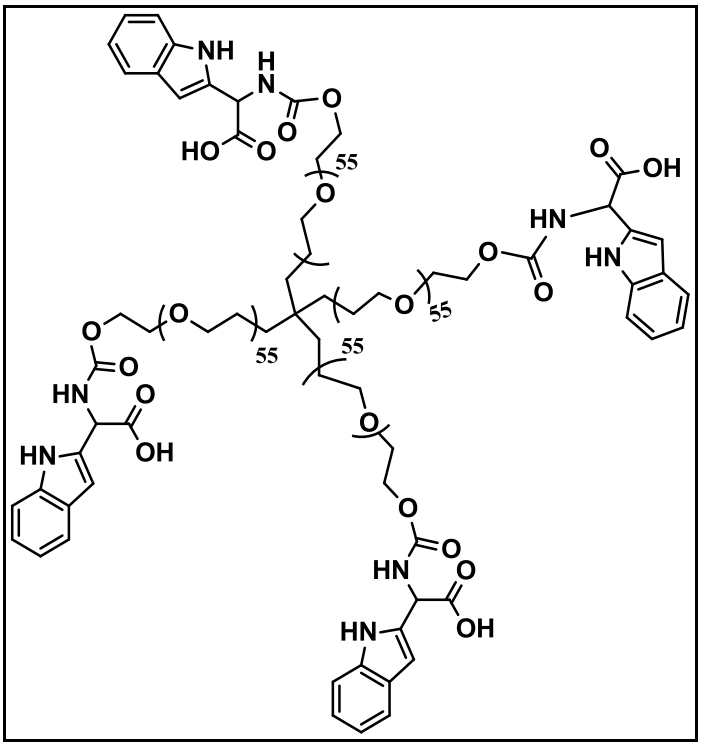

Figure 2.6. Molecular structure of PEG-(Trp)$_4$

2.2.6. Synthesis of (H-N-Boc)$_2$-PEG-(OH)$_2$

In an ice bath $(NH_2)_2$-PEG-$(OH)_2$ (10,000 g/mol) (200 mg, 20x10^{-3} mmol) and di-tert-butyl dicarbonate (9.8 mg, 45x10^{-3} mmol) were put into a mixture of dioxane:water (1:1) (3.2 ml). Next, triethyl amine (8.6 µL) was added into the mixture and it was stirred under argon atmosphere for 30 min. After that the mixture was stirred at 25 ^{o}C for 17 hours. At the end of the reaction, the mixture was extracted with ethyl acetate (70 ml) and the pH of the organic phase was adjusted to 1 by HCl (1N) and back extracted wit ethyl acetate (70 ml) for 3 times. Combined organic phases were dried over Na_2SO_4. Organic solvent was evaporated to afford (H-N-Boc)$_2$-PEG-$(OH)_2$ (Figure 2.7) as white powder (183.6 mg, 90% yield) (Giorgioni et al., 2010). In the NMR spectrum of this molecule (Figure A.5, appendix) the integration of amide protons of polyethylene glycol (4H) was

taken as reference. The signal of protected group was observed at 1.42 ppm as 18 protons. So the NMR spectrum of the molecule proved that the molecule was synthesized. Proton NMR signals of molecule were observed at following ppm values; ^{1}H NMR (400 MHz, $CDCl_3$) δ: 5.08 (t, 4H), 3.80 (t, 4H), 3.67-3.50 (m, 896H), 3.45 (t, 4H), 3.29 (t, 4H), 1.42 (s, 18H).

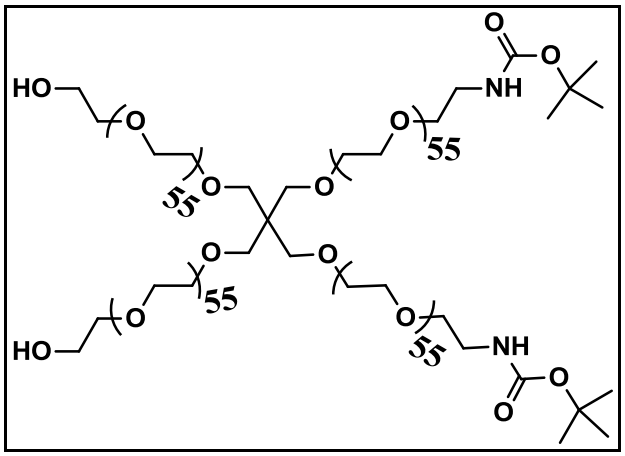

Figure 2.7. Molecular structure of (H-N-Boc)$_2$-PEG-(OH)$_2$

2.2.7. Synthesis of (H-N-Boc)$_2$-PEG-(p-nitrophenyl carbonate)$_2$

(H-N-Boc)$_2$-PEG-(OH)$_2$ (148 mg, 14.5x10^{-3} mmol) and p-nitrophenyl chloroformate (17.3 mg, 86.3x10^{-3} mmol) were mixed in dry DCM (2 ml) under argon atmosphere. Next dry triethyl amine (9 μL) was added into the mixture and it was stirred at 25 ^{o}C for 24 hours. At the end of the experiment TFA was added into the experiment until the color of the experiment turned to colorless from yellow. After that the solvent was evaporated at rotary and the crude product precipitated in cold diethyl ether for 3 times to afford (H-N-Boc)$_2$-PEG-(p-nitrophenyl carbonate)$_2$ (Figure 2.8) as white powder (129 mg, 85% yield) (Mueller at al., 2011). In the NMR spectrum of this molecule (Figure A.6, appendix) the signal of protected group was taken as refence (18 H). The proton signals of p-nitrophenyl chloroformate at 8.30 ppm (4H) and 7.55 ppm (4H) proved that the p-nitrophenyl chloroformate molecule made bond with the polymer. Proton NMR signals of molecule were observed at following ppm values; ^{1}H NMR (400 MHz, DMSO-d_6) δ: 8.30 (d, 4H), 7.55 (d, 4H), 7.11 (s, 4H), 7.09 (t, 4H), 6.94 (t, 4H), 4.14-4.09 (m, 8H), 3.48 (m, 896H), 3.13 (d, 8H).

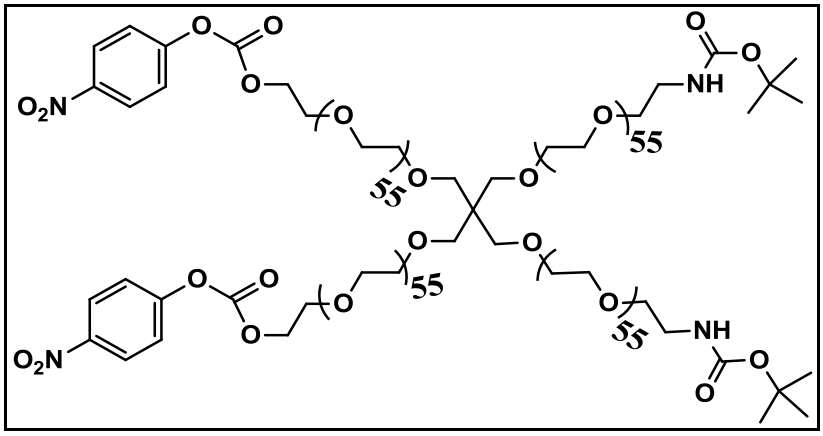

Figure 2.8. Molecular structure of (H-N-Boc)$_2$-PEG-(p-nitrophenyl carbonate)$_2$

2.2.8. Synthesis of (H-N-Boc)$_2$-PEG-(Trp)$_2$

(H-N-Boc)$_2$-PEG-(p-nitrophenyl carbonate)$_2$ (147 mg, 13.8x10^{-3} mmol) and tryptophane (56.3 mg, 276x10^{-3} mmol) were mixed in dry dimethyl sulfoxide (DMSO) (2 ml) under argon atmosphere at 25 ^{o}C for 5 hours. Afterwards the experiment was cooled to 0 ^{o}C and the pH of the experiment was arranged to 3 by HCl (2 M) solution. Next the crude product was extracted with distilled water for 6 times and dried over Na_2SO_4. Finally solvent was evaporated at rotary and the product precipitated in cold diethyl ether for 3 times to afford (H-N-Boc)$_2$-PEG-(Trp)$_2$ (Figure 2.9) as white powder (114 mg, 78% yield) (Mueller et al., 2011). In the NMR spectrum of the molecule (Figure A.7, appendix) the signal of protected group was taken as refence (18 H). The signal at 10.74 ppm (2H) proved that the tryptophan molecule made bond with the polymer. Also other proton signals of the tryptophan were observed at NMR spectra with expected integral ratios and this proved that the molecule was synthesized. Proton NMR signals of molecule were observed at following ppm values; ^{1}H NMR (400 MHz, DMSO-d_6) δ:10.74 (s, 2H), 7.49 (d, 2H), 7.30 (d, 2H), 7.09 (s, 2H), 7.02 (t, 2H), 6.94 (t, 2H), 6.70 (s, 2H), 3.96 (t, 2H), 3.48 (m, 896H), 3.03 (t, 4H), 1.35 (s, 18H).

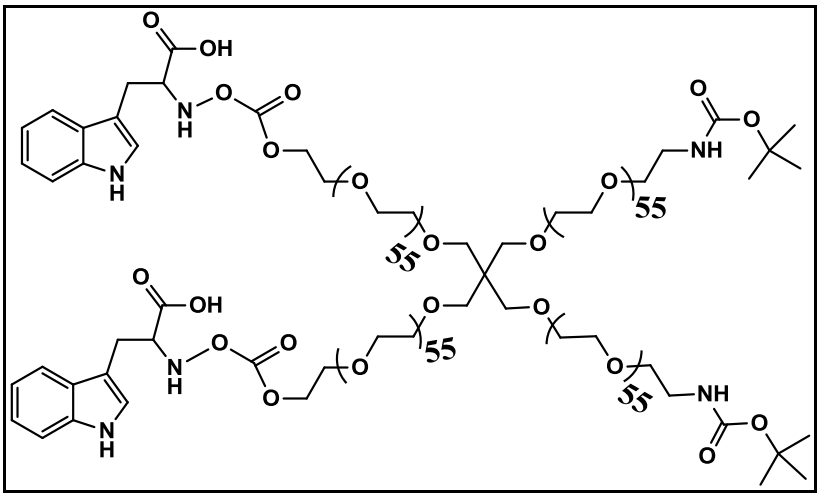

Figure 2.9. Molecular structure of $(H\text{-}N\text{-}Boc)_2$-PEG-$(Trp)_2$

2.2.9. Synthesis of $(NH_2)_2$-PEG-$(Trp)_2$

$(H\text{-}N\text{-}Boc)_2$-PEG-$(Trp)_2$ (114 mg, $10.7x10^{-3}$ mmol), TFA (0.5 ml) and DCM (2 ml) were stirred at 25 ^oC for 3 hours. At the end of the experiment the solvents were evaporated at rotary evaporator. The crude product was precipitated in cold diethyl ether for 4 times to afford (Figure 2.10) as white powder (95.1 mg, 85% yield) (Lee et al., 2002). 18 proton of protected group at 1.35 ppm was not observed in NMR spectrUM (Figure A.7, appendix) of the molecule and other proton signals of the molecule was observed as it was expected. So this proved that the molecule was synthesized. Proton NMR signals of molecule were observed at following ppm values; ^1H NMR (400 MHz, DMSO-d_6) δ:10.95 (s, 2H), 7.69 (s, 2H), 7.50 (d, 2H), 7.31 (d, 2H), 7.13 (s, 2H), 7.04 (t, 2H), 6.96 (t, 2H), 4.19-4.15 (m, 4H), 3.99-3.95 (m,4H), 3.49 (m, 896H), 2.96 (t, 8H).

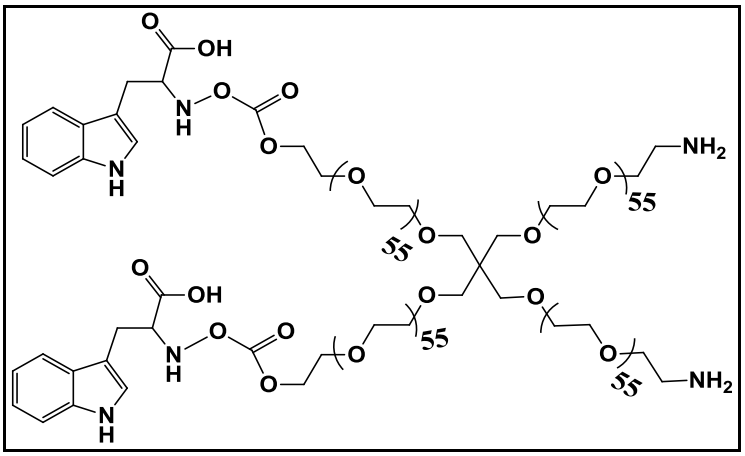

Figure 2.10. Molecular structure of (H-N-Boc)$_2$-PEG-(Trp)$_2$

2.2.10. Synthesis of (N-Boc-L-DOPA)$_2$-PEG-(Trp)$_2$

$(NH_2)_2$-PEG-$(Trp)_2$ (92 mg, $8.81x10^{-3}$ mmol), N-Boc-L-DOPA (11 mg, $35.3x10^{-3}$ mmol), 1-hydroxybenzotriazol (HOBT) (7.8 mg, 0.057 mmol), and triethyl amine (13.3 µL) were mixed in a mixture of DCM (460 µL) and DMF (460 µL) at 25 ^oC until all compunds dissolved. After that 2-(1H-benzotriazol-1-yl)-1,1,3,3-tetramethyluronium hexafluorophosphate (HBTU) (13.28 mg, 0.035 mmol) and DCM (460 µL) were added into the mixture and it was stirred at 25 ^oC under argon atmosphere for 5 hours. At the end of the experiment ninhydrin test was applied to control whether there is any primary amine in the experiment medium , 2-3 drops of product was dissolved in DCM (1 ml) and 2-3 drops of ninhydrin solution was put into this mixture. The mixture was stirred at 50 ^oC for 30 min, the test result was negative. The crude product was washed with saturated sodium chloride solution (50 ml), $NaHCO_3$ (5% w/ml) solution, HCl (1 M) solution (50 ml), and distilled water (50 ml). The organic phase was dried over Na_2SO_4 and the product was precipitated in cold diethyl ether for 3 times to afford (N-Boc-L-DOPA)$_2$-PEG-$(Trp)_2$ (Figure 2.11) as white solid (66.5 mg, 70% yield) (Lee et al., 2002). In the NMR spectrum of this molecule (Figure A.9, appendix) the integration of methylene protons of polyethylene glycol (896H) was taken as reference and the proton signal of N-Boc-L-DOPA was observed at 1.29 ppm (18 H). Also other protons on the synthesized molecule gave signal at expected ppm and with expected integration values. So it was proved that the molceule was sytnesized. Proton NMR signals of molecule were observed at following ppm values; ^1H NMR (400 MHz, DMSO-d_6) δ: 7.49 (d, 2H), 7.29 (d, 2H), 7.11-7.09 (m, 2H), 7.044-7.007 (m, 2H), 6.99-6.92 (m, 2H), 6.80-6.78 (m,4H), 6.58-6.55 (m,

2H), 6.54-6.43 (m, 2H), 3.99-3.92 (m, 10H), 3.48 (896H), 3.20-3.17 (m, 8H), 2.99 (t, 4H), 1.29 (s, 18H).

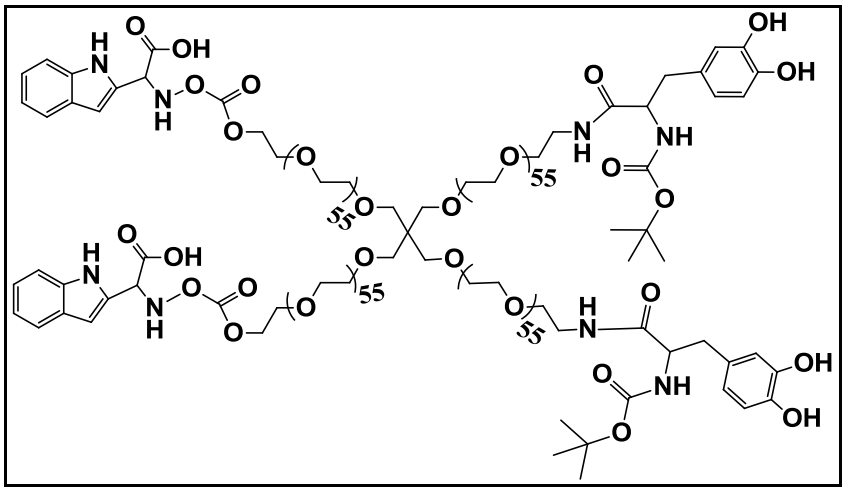

Figure 2.11. Molecular structure of $(N\text{-Boc-L-DOPA})_2$-PEG-$(Trp)_2$

2.2.11. Synthesis of $(DOPA)_2$-PEG-$(Trp)_2$

$(N\text{-Boc-L-DOPA})_2$-PEG-$(Trp)_2$ (66.5 mg, 6.16×10^{-3} mmol) was dissolved in DCM (2 ml), and TFA (200 µL) was added. The mixture was stirred at 25 ^{o}C for an hour. After evaporating the solvent at rotary the crude product was precipitated in cold diethyl ether for 3 times to afford $(DOPA)_2$-PEG-$(Trp)_2$ (Figure 2.12) as white solid (58.5 mg, 90% yield) (Lee et al., 2002).

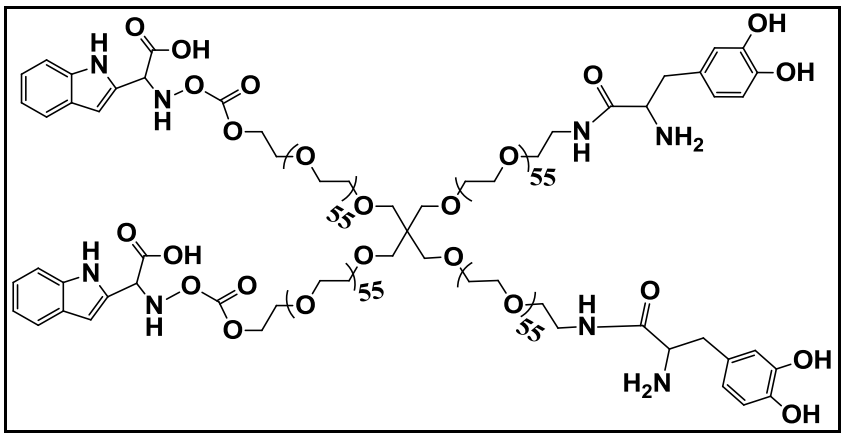

Figure 2.12. Molecular structure of $(DOPA)_2$-PEG-$(Trp)_2$

2.2.12. Synthesis of Spin Labeled Polystyrene (SLPS)

Tempo-4-carboxylate (250 µL, 10 mM) in MES buffer (0.2 M) at pH 3.0 was mixed with amine modified polystyrene bead (100 µL) in the presence of cross-linker, 1-ethyl-3-(3-dimethylaminopropyl) carbodiimide (EDC) (90 µL, 38 mM) for 24 hours at 29 ^{o}C (Figure 2.13). EDC and free Tempo-4-carboxylate were washed out for several times with MES buffer, pH 3.0. (Akdogan et al. 2014)

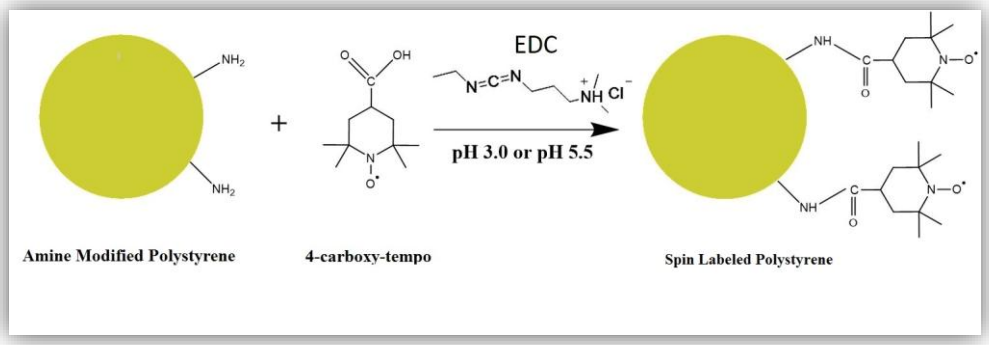

Figure 2.13. Synthesis of SLPS

2.2.13. Synthesis of Spin Labeled Silica (SLSi)

Tempo-4-carboxylate (250 µL, 10 mM) in MES buffer (0.2 M) at pH 3.0 was mixed with amine modified silica bead (100 µL) in the presence of cross-linker, 1-ethyl-3-(3-dimethylaminopropyl) carbodiimide (EDC) (90 µL, 38 mM) for 24 hours at 22 ^{o}C (Figure 2.14). EDC and free Tempo-4-carboxylate were washed out for several times with MES buffer, pH 3.0. (Akdogan et al. 2014)

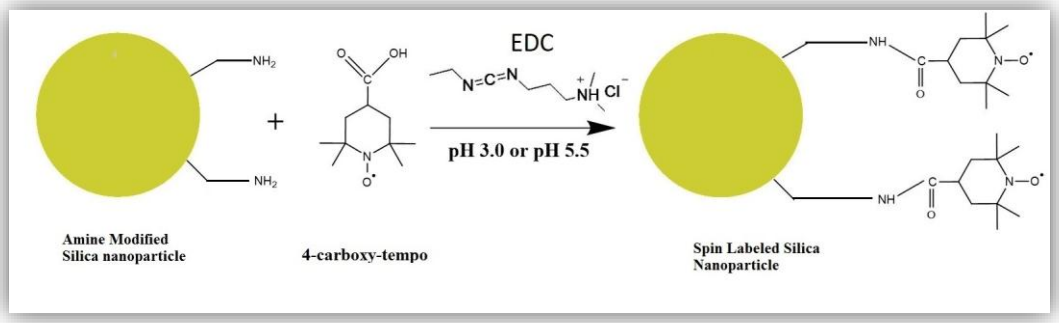

Figure 2.14. Synthesis of SLSi

2.2.14. Synthesis of PEG-$(DOPA)_4$ Hydrogel by Fe^{3+} Ion

PEG-$(DOPA)_4$ (15 mg, $1.36x10^{-3}$ mmol) was dissolved in sodium hydroxide (NaOH) solution (40 µL, 0.5 M). Next $Fe_2Cl_3 \cdot 6H_2O$ (2.2 mg, $6.8x10^{-3}$ mmol) was dissolved in sodium hydroxide solution (100 µL, 0.5 M) and 13.3 µL of this solution was put into PEG-$(DOPA)_4$ solution and they mixed with vortex. After that NaOH solution (26 µL, 0.5 M) was added into the mixture and it was mixed for 15 seconds with vortex. After 5 minutes formation of hydrogel was observed. (Krogsgaard et al., 2013)

2.2.15. Synthesis of $(DOPA)_2$-PEG-$(Trp)_2$ Hydrogel by Fe^{3+} Ion

$(DOPA)_2$-PEG-$(Trp)_2$ (29.4 mg, $2.72x10^{-3}$ mmol) was dissolved in sodium hydroxide (NaOH) solution (40 µL, 0.5 M). Next $Fe_2Cl_3 \cdot 6H_2O$ (2.2 mg, $6.8x10^{-3}$ mmol) was dissolved in sodium hydroxide solution (100 µL, 0.5 M) and 13.3 µL of this solution was put into $(DOPA)_2$-PEG-$(Trp)_2$ solution and they mixed with vortex. After that NaOH solution (26 µL, 0.5 M) was added into the mixture and it was mixed for 15 seconds with vortex. After 15 minutes formation of hydrogel was observed. (Krogsgaard et al., 2013)

2.2.16. Synthesis of PEG-$(DOPA)_4$ Hydrogel by $(IO_3)^-$ Ion

KIO_3 (2.1 mg, $0.89x10^{-3}$ mmol) was dissolved in 890 µL MES buffer (0.2 M, pH=3.0). After that 28 µL of this solution was mixed with PEG-$(DOPA)_4$ (2.5 mg, $0.23x10^{-3}$ mmol). The color of the solution turned to yellow immediately. After 30 min formation of gel was observed. (Mirshafian et al., 2016)

CHAPTER 3

RESULTS AND DISCUSSION

3.1 Characterization of SLPS and SLSi by ESR Spectroscopy

Spin labeled polystyrene (SLPS) and spin labeled silica (SLSi) were tested by ESR spectroscopy. The dynamic properties of spin label can be understood from the ESR spectrum of spin label. If the rotational motion of the spin label is fast, the spectrum has sharp signals. On the other hand, if the rotational motion is slow the spectrum has broad signals. So when the spectrum has broad signals, it shows that the spin label is bound to nanoparticles (Figure 3.1, 3.2). Furthermore, spectrum has not any sharp signals which means that the free spin labels were washed completely.

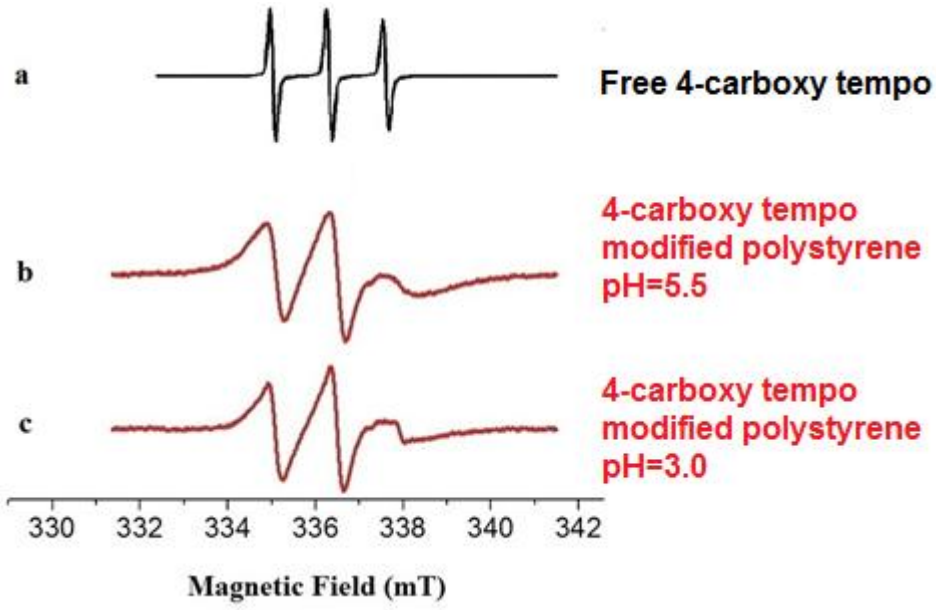

Figure 3.1. ESR spectra of (a) free 4-carboxy Tempo label in MES buffer (0.2 M, pH=3.0), (b) 4-carboxy Tempo label bonded with polystyrene nanoparticle in MES buffer (0.2 M, pH=3.0), (c) 4-carboxy Tempo label bonded with polystyrene nanoparticle in MES buffer (0.2 M, pH=5.5).

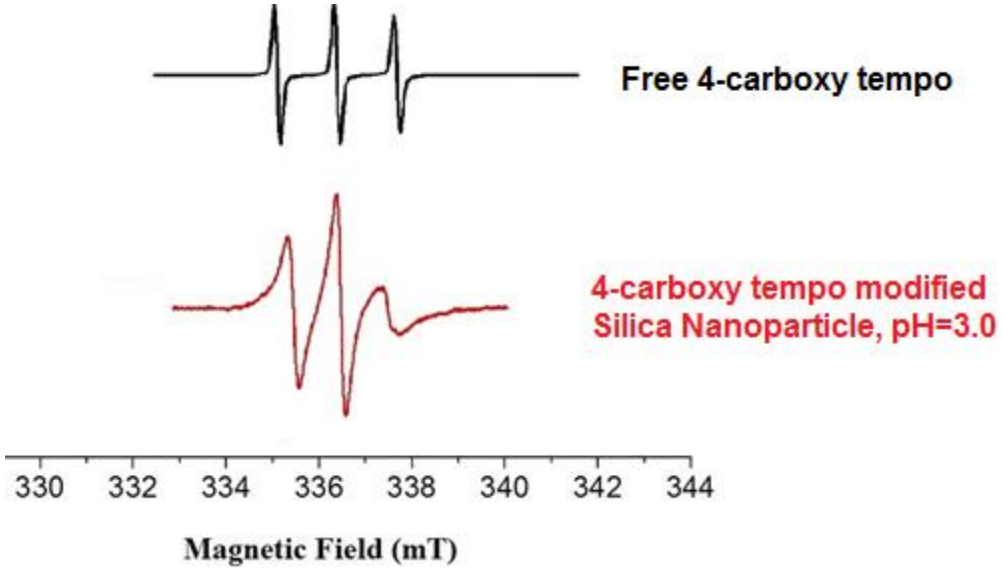

Figure 3.2. ESR spectra of free 4-carboxy Tempo label in MES buffer (0.2 M, pH=3.0) (black), 4-carboxy tempo label bonded with silica nanoparticle in MES buffer (0.2 M, pH=3.0) (red).

3.2. Application of ESR Spectroscopy on Adhesion Studies

Adhesion of the synthesized polymers to hydrophobic spin labeled polystyrene (SLPS) and to hydrophilic spin labeled silica (SLSi) nanoparticles were tested by ESR spectroscopy. Since $(Trp)_2$-PEG-$(DOPA)_2$ and PEG-$(Trp)_4$ did not adhere to SLPS surface, they were not used for adhesion measurements with SLSi. SLSi has hydrophilic surface and therefore it is not expected to adhere these two polymers to SLSi surface. For each ESR measurement the volumetric ratio of samples (SLPS: Polymer) was 2:1. Each sample was stirred 1 minute by vortex for 2 times by 5 min interval after mixing.

3.2.1. Adhesion Study of PEG-$(DOPA)_4$ to SLPS and SLSi Surface

ESR results showed that PEG-(N-Boc-L-$DOPA)_4$ adheres to SLPS. This adhesion is stronger at pH 3.0 than the adhesion at pH 5.5 (Figure 3.3) because at pH 3 the change of line shape of ESR signal from sharp to broad is higher compared to change at pH 5.5. It's well known that DOPA can be oxidized easily at higher pH values and also oxidation of DOPA reduces its adhesion ability. Therefore at pH=5.5 the adhesion ability of PEG-$(DOPA)_4$ is weaker than the adhesion ability of PEG-$(DOPA)_4$ at pH=3.The ESR

spectrum of mixture of SLPS and PEG-$(DOPA)_4$ shows a broad signal in low field (Figure 3.3, red signals), but when there was no PEG-$(DOPA)_4$ in the medium, the spectrum had sharper signal in low field (Figure 3.3, black signals). PEG-$(DOPA)_4$ did not adhere to SLSi surface as it was expected (Figure 3.4), because SLSi has hydrophilic surface. Since it is covered with strong hydration layers, the polymers cannot pass these layers to adhere to the surface.

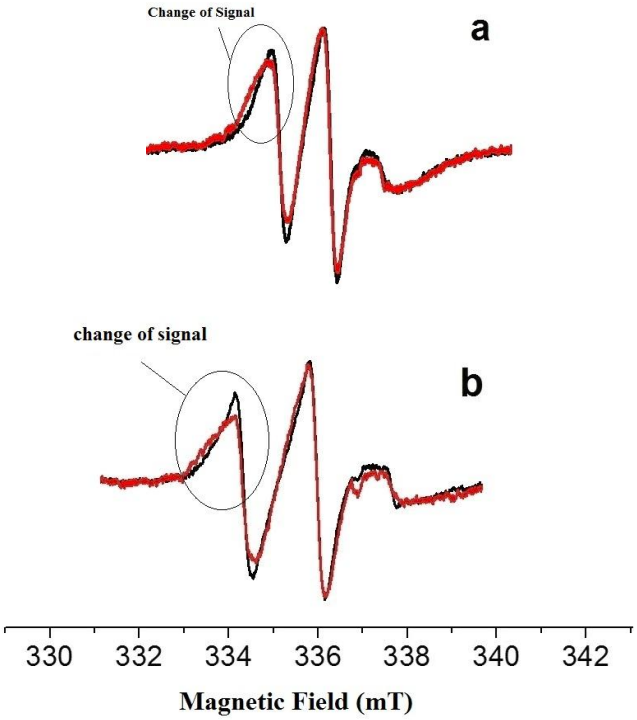

Figure 3.3. (a) ESR spectra of SLPS at pH 5.5 (black) and after adhesion of PEG-$(DOPA)_4$ (5.1 µM, 90 mg/mL) to SLPS. (b) ESR spectra of SLPS at pH 3.0 (black) and after adhesion of PEG-$(DOPA)_4$ (5.1 µM, 90 mg/mL) to SLPS

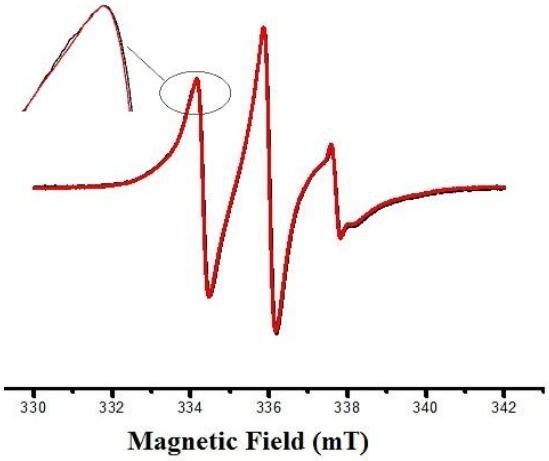

Figure 3.4. ESR spectra of SLSi (black), and after adhesion of PEG-$(DOPA)_4$ (5.1 µM, 90 mg/mL) to SLSi surface (red).

Adhesion of the PEG-$(DOPA)_4$ was better at pH 3.0 because when the pH increases hydroxyl groups of DOPA are oxidized to ortho quinone. The adhesive property of DOPA ortho quinone is not as good as DOPA hydroxyl. Therefore, ESR measurements of the other synthesized polymers were done at pH 3 in the MES buffer (0.2 M).

3.2.2. Adhesion Study of PEG-$(Trp)_4$ to the SLPS Surface

PEG-$(Trp)_4$ did not show any adhesion to SLPS because it has no DOPA groups in its chemical structure. Therefore, the ESR signal of the mixture of SLPS and PEG-$(Trp)_4$ is very similar to the ESR signal of SLPS (Figure 3.5).

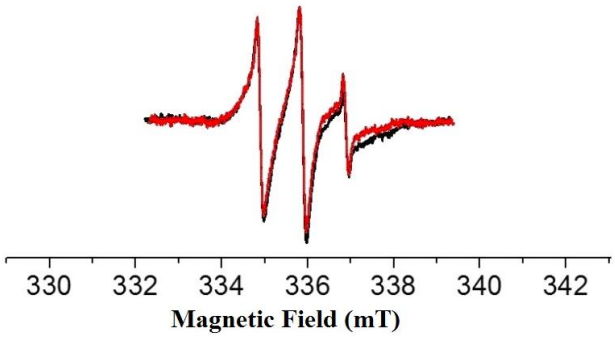

Figure 3.5. ESR spectrum of SLPS at pH 3.0 (black) and ESR spectrum of SLPS after addition of PEG-$(Trp)_4$ (5.1 µM, 90 mg/mL) to SLPS at pH 3.0 (red).

3.2.3. Adhesion Study of $(DOPA)_2$-PEG-$(Trp)_2$ to the SLPS Surface

$(DOPA)_2$-PEG-$(Trp)_2$ did not show any adhesion to SLPS, because it has less DOPA groups in its molecular structure compare to the PEG-$(DOPA)_4$. Hence, there was no variation on the ESR spectrum of SLPS after addition of $(DOPA)_2$-PEG-$(Trp)_2$ to SLPS (Figure 3.6).

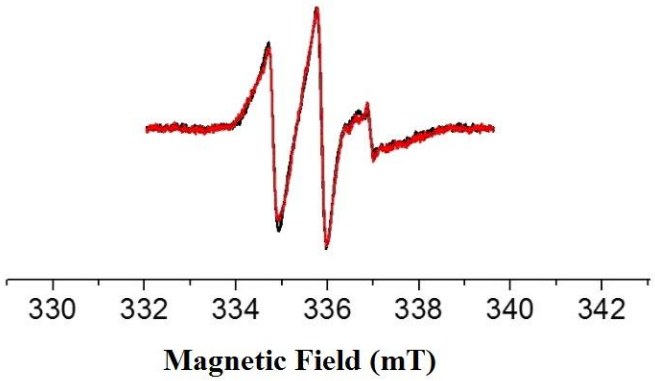

Figure 3.6. ESR spectrum of SLPS at pH 3.0 (black) and ESR spectrum of mixture of SLPS and $(DOPA)_2$-PEG-$(Trp)_2$ (5.1 µM, 90 mg/mL) at pH 3.0 (red).

3.3. UV-Vis and ESR Measurements of Fe^{3+} Made of Hydrogels

Adhesive and cohesive property of gel form of DOPA modified polymers are better compare to their molecular form so the gel form was prepared (Sever et al., 2004). UV-Vis spectra of gel form of PEG-$(DOPA)_4$ and $(DOPA)_2$-PEG-$(Trp)_2$ showed the presences of -bis and -tris complexes of catechol groups of DOPA molecules that formed by Fe^{3+} ions. -Bis complex is formed at pH between 5.0 and 10.8, -tris complex is formed at pH between 10.8 and 12.00. The obtained gels did not adhere to hydrophobic SLPS surface and to hydrophilic SLSi surface.

3.3.1. UV-Vis Measurements of Fe^{3+} Based Gel Form of PEG-$(DOPA)_4$

PEG-$(DOPA)_4$ has absorbances at 590 nm for -bis complex and at 490 nm for -tris complex (Krogsgaard et al., 2013) While the absorbance of -bis complex is decreasing, the absorbance of -tris complex is increasing with increasing pH value (Figure 3.7). This shows that tris- complex gel formation is favoured at higher pH values.

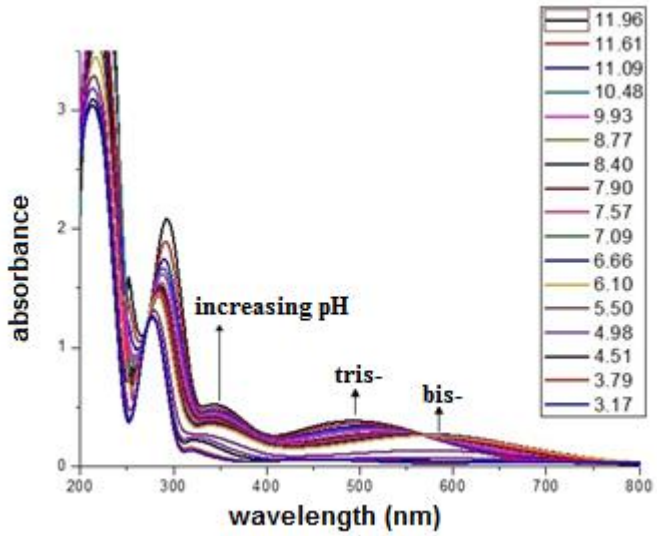

Fiure 3.7. UV-Vis spectra of gel form of PEG-$(DOPA)_4$ (24 μM) with Fe^{3+} (6 μM) at different pH.

Gel form of PEG-$(DOPA)_4$ was cut in to two pieces with a spatula and after 5 min the pieces came together, results of the crosslinking between DOPA and Fe^{3+} (Figure 3.8).

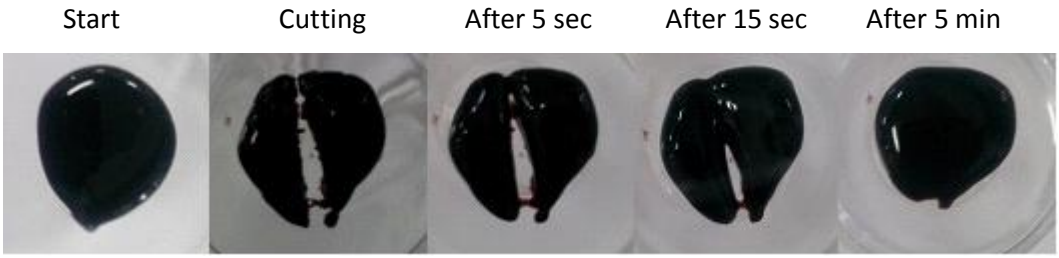

Figure 3.8. Gel form of PEG-$(DOPA)_4$ (17 mM) with Fe^{3+} (22.7 mM) at pH 9 in NaOH solution (0.5 M).

3.3.2. UV-Vis Measurements of Fe^{3+} Based Gel Form of $(DOPA)_2$-PEG-$(Trp)_2$

$(Trp)_2$-PEG-$(DOPA)_2$ had absorbances at the same wave lengths (590 nm for -bis complex and at 490 nm for -tris complex) with PEG-$(DOPA)_4$ (Figure 3.9), because both of them have DOPA catechol groups in their chemical structures. However the intensity of absorbances of $(Trp)_2$-PEG-$(DOPA)_2$ were lower than PEG-$(DOPA)_4$ because the number of DOPA catechol groups in a $(Trp)_2$-PEG-$(DOPA)_2$ (Figure 2.10) is half of the number of DOPA catechol groups in a PEG-$(DOPA)_4$ (Figure 2.2) molecule .

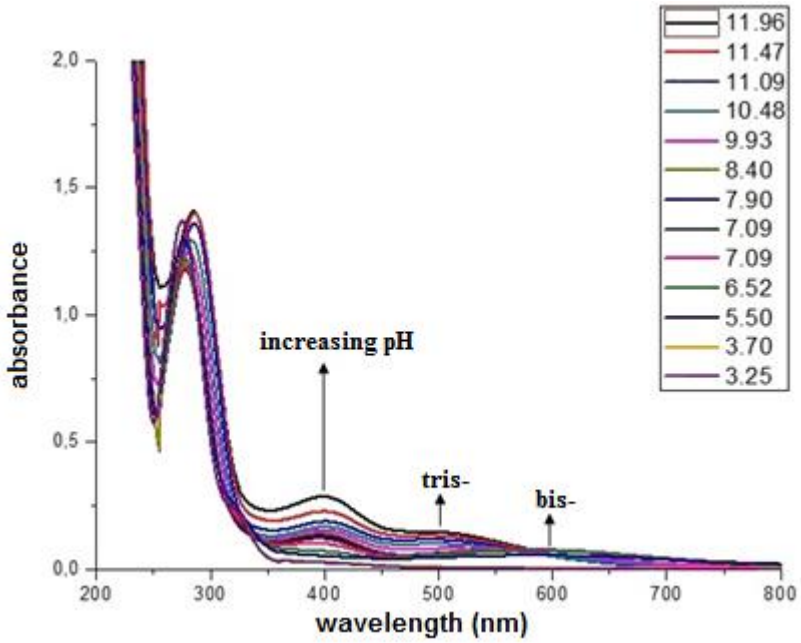

Figure 3.9. UV-Vis spectra of gel form of $(DOPA)_2$-PEG-$(Trp)_2$ (24 μM) with Fe^{3+} (3 μM) at different pH.

Gel form of $(DOPA)_2$-PEG-$(Trp)_2$ was cut into two pieces with a spatula and after 15 min the pieces came together due to the cross linking of DOPA hydroxyl (-OH) groups with Fe^{3+} (Figure 3.9). Unlike gel formation of PEG-$(DOPA)_4$, it took longer time to became a gel for $(DOPA)_2$-PEG-$(Trp)_2$ (Figure 3.10).

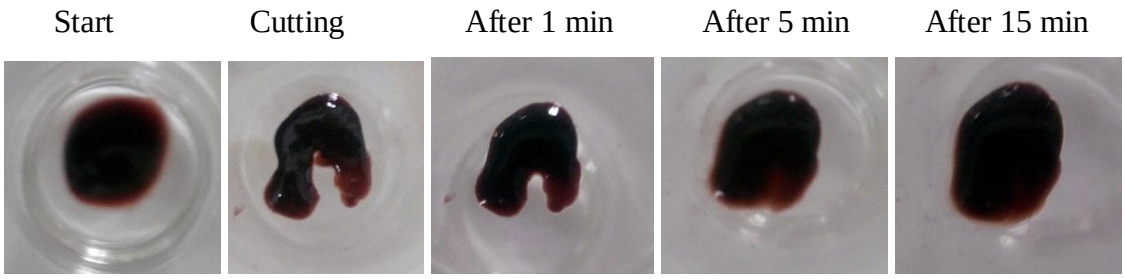

Figure 3.10. Gel form of $(DOPA)_2$-PEG-$(Trp)_2$ (34 mM) with Fe^{3+} (22.7 mM) at pH 9 in NaOH solution (0.5 M).

3.3.3. Adhesion Study of Fe^{3+} Based Gel Form of PEG-$(DOPA)_4$ and $(Trp)_2$-PEG-($DOPA)_2$ to the SLPS Surface

Different than adhesion of PEG-$(DOPA)_4$ molecule, the gel form of PEG-$(DOPA)_4$ did not show any adhesion to SLPS (Figure 3.12) because the DOPA groups in gel form are oxidized to ortho quinone at high pH (Figure 3.11). Therefore, the number of hydroxyl group decreases and the resulting crosslinking structure is not strong enough to have strong adhesion. In addition, gel form of $(DOPA)_2$-PEG-$(Trp)_2$ did not adhere to surface of SLPS (Figure 3.13), because it has less DOPA hydroxyl groups and also it has tryptophan molecules which has no hydroxyl groups on its structure (Figure 2.11). So the cross linking and adhesion properties of these gels are not as good as those of PEG-$(DOPA)_4$ molecule.

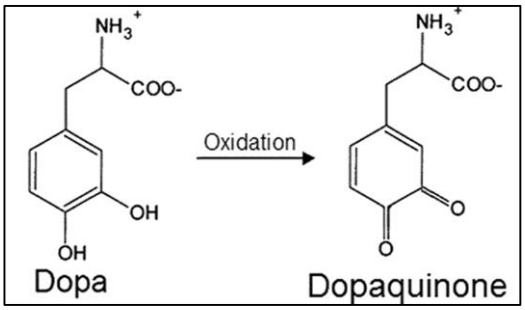

Figure 3.11. Oxidation of DOPA catechol group to DOPA quinone

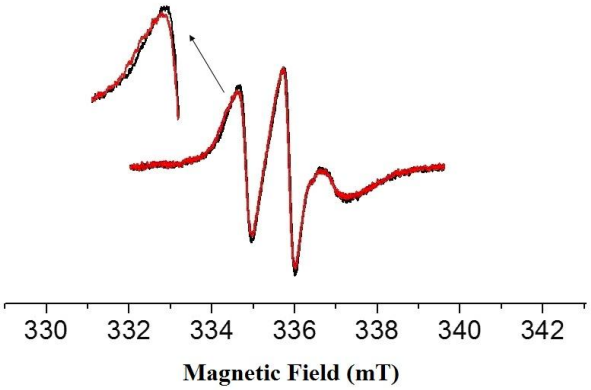

Figure 3.12. ESR spectra of SLPS at pH 3.0 (black) and ESR spectra of mixture of SLPS and gel form of PEG-$(DOPA)_4$ at pH 3.0 (red).

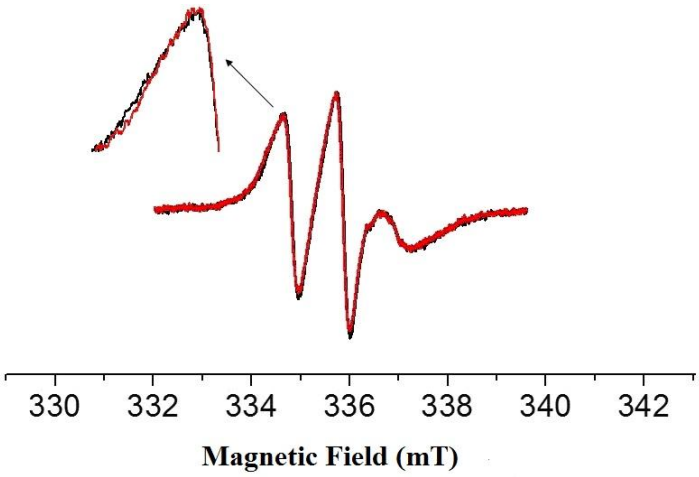

Figure 3.13. The ESR spectrum of SLPS at pH 3.0 (black), the ESR spectrum of mixture of SLPS and gel form of $(DOPA)_2$-PEG-$(Trp)_2$ (5.1 μM, 90 mg/mL) on SLPS at pH 3.0 (red).

3.4. UV-Vis and ESR Measurements of $[IO_3]^-$ Made of Hydrogel

3.4.1. UV-Vis Measurements of $[IO_3]^-$ Based Gel Form of PEG-$(DOPA)_4$

Addition of KIO_3 to PEG-$(DOPA)_4$ solution in MES buffer (0.2 M, pH=3.0) showed an immediate color change from colorless to yellow. It is the signature color of o-quinone (Figure 3.14) (λ_{max}= 400 nm).

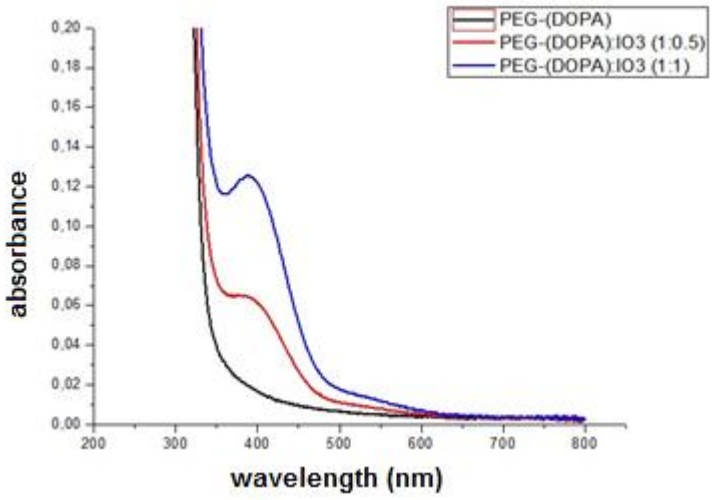

Fiure 3.14. UV-Vis spectra of PEG-$(DOPA)_4$ (24 μM) in MES buffer (0.2M, pH=3.0) (black), gel form of PEG-$(DOPA)_4$ (24 μM) with $[IO_3]^-$ (12 μM) in MES buffer (0.2M, pH=3.0) (red), gel form of PEG-$(DOPA)_4$ (24 μM) with IO_3^- (24 μM) in MES buffer (0.2M, pH=3.0) (blue).

Gel form of PEG-$(DOPA)_4$ showed an dark yellow color when the mol ratio of $[IO_3]^-$ ion and DOPA is 1:1, while the color was light yellow when the mol ratio of $[IO_3]^-$ ion and DOPA is 0.5:1 (Figure 3.15). The reason is the number of o-quinone structures that occur with addition of $[IO_3]^-$ ions. The more o-quinone in the structure the darker the color for hydrogel.

Figure 3.15. Gel form of PEG-$(DOPA)_4$ (8 mM) with IO_3^- (32 mM) in MES buffer (0.2 M, pH=3.0) (left), PEG-$(DOPA)_4$ (8 mM) with $[IO_3]^-$ (16 mM) in MES buffer (0.2 M, pH=3.0) (right).

3.4.2. Adhesion Study of $[IO_3]^-$ Based Gel Form of PEG-$(DOPA)_4$ to SLPS Surface

$[IO_3]^-$ based gel form of PEG-$(DOPA)_4$ showed strong adhesion to SLPS surface compare to Fe^{3+} based gel form and molecule form of PEG-$(DOPA)_4$. The ESR spectrum of $[IO_3]^-$ based gel had broader low field signal compared to the low field signal of SLPS. When the ratio of DOPA to $[IO_3]^-$ is 1:1 the adhesion is stronger (Figure 3.16) compared to the Fe based gel and PEG-$(DOPA)_4$ molecules (Figure 3.12).

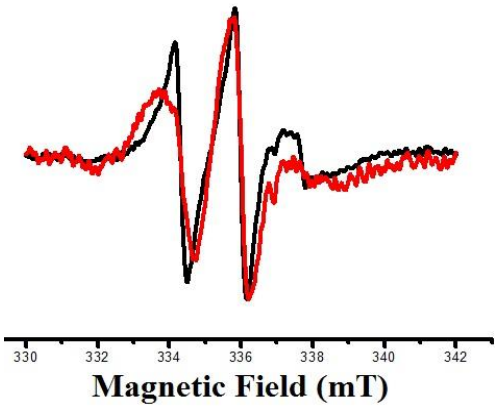

Figure 3.16. ESR spectrum of SLPS at pH 3.0 (black), and ESR spectrum of mixture of SLPS and IO_3^- ion based gel form of PEG-$(DOPA)_4$ (5.1 µM, 90 mg/ml) pH 3.0 (red). (The ratio of DOPA: IO_3^- is 1:1)

3.4.3. Adhesion Study of $[IO_3]^-$ Based Gel Form of PEG-$(DOPA)_4$ to SLSi Surface

$[IO_3]^-$ based gel form of PEG-$(DOPA)_4$ did not show any adhesion to SLSi surface (Figure 3.17). The reason is the hydrophilic surface character of SLSi. Strong hydration layers around the silica nanoparticles prevent polimer adhesion.

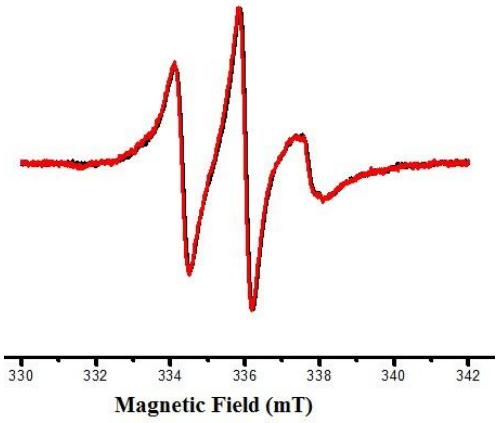

Figure 3.17. ESR spectrum of SLSi at pH 3.0 (black), and ESR spectrum of mixture of SLSi and IO_3^- ion based gel form of PEG-$(DOPA)_4$ (5.1 μM, 90 mg/ml) at pH 3.0 (red). (The ratio of DOPA: IO_3^- is 1:1)

3.4.4. ESR Measurements of Mixture of Free 4-carboxy tempo and $[IO_3]^-$ Based Gel Form of PEG-$(DOPA)_4$

In order to control the viscosity effect on ESR lineshape, we measured the 4-carboxy tempo radical in the gel form of PEG-$(DOPA)_4$. When the PEG-$(DOPA)_4$ molecules turned to gel form the viscosity of medium increases. So the rotational motion of the radicals can be affected by the viscosity. However, ESR results showed that the viscosity did not affect the rotational motion of 4-carboxy tempo radical (Figure 3.18). Therefore, the ESR spectra of free 4-carboxy tempo radical in MES buffer and the mixture of radical with gel form of PEG-$(DOPA)_4$ were same.

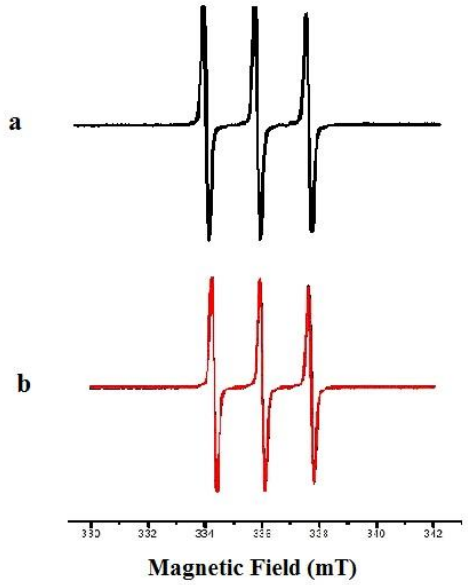

Figure 3.18. a) ESR spectra of 4-carboxy tempo radical (0.6 mM) in MES buffer at pH 3.0 (black), (b) ESR spectrum of mixture of gel form of PEG-$(DOPA)_4$ (32 mM) (Ratio of DOPA to IO_3^-, 1:1) and 4-carboxy tempo radical.

3.5. Adhesion Measurements of Bovine Serum Albumin (BSA) to SLSi Surface

Bovine serum albumin (BSA) has a strong adhesion to surface of SLPS (Akdogan et al., 2014). Hydrophobic surface of polystyrene (PS) has a lower hydration shell therefore BSA can attach to the surface of PS. BSA is a protein with a 66 kDa molecular weight and especially its open structure binds to SLPS very efficiently (Akdogan et al., 2014). However, BSA did not adhere to SLSi surface (Figure 3.19). The ESR spectra of both SLSi and the mixture of BSA and SLSi were same. Hydrophilic surface of silica nanoparticles causes a strong hydration shell and this prevents the adsorption of BSA to silica surface. So we made the following adhesion measurements in order to show that even a molecule (BSA) which has a powerfull adhesion property can not adhere to surface of SLSi nanoparticle.

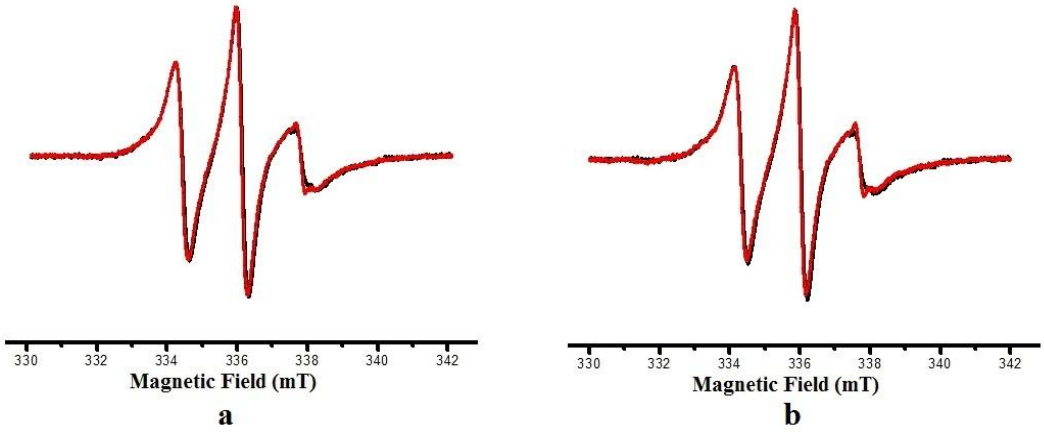

Figure 3.19. a) ESR spectra of SLSi (black) and the mixture of SLSi with BSA (2.5 mg/ml) (red), (b) ESR spectra of SLSi (black) and the mixture of SLSi with BSA (30 mg/ml) (red).

BSA unfolds when 5 M of urea mixed with BSA, therefore hydrophobic amino acids in BSA can access to the surface, too. According to ESR measurements unfolded BSA did not adhere to SLSi surface (Figure 3.20).

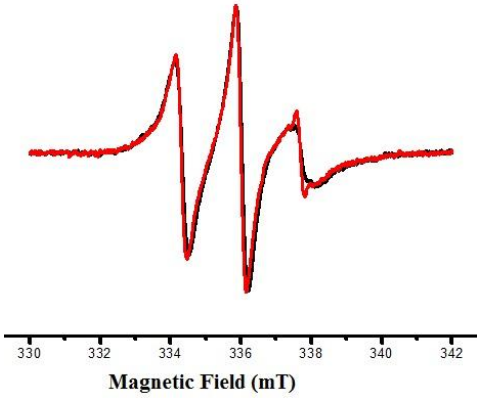

Figure 3.20. ESR spectrum of SLSi (black) and the mixture of SLSi with BSA (2.5 mg/ml) in urea solution (5 M) (red).

CHAPTER 4

CONCLUSION

In summary, using ESR spectroscopy we demonstrated that PEG-$(DOPA)_4$ molecules adhere to wet spin label polystyrene (SLPS) without applying an external force. However, $(DOPA)_2$-PEG-$(Trp)_2$ and PEG-$(Trp)_4$ did not show any adhesion to the surfaces. It could be concluded that if the number of DOPA molecule increases the adhesion of polymer increases.

Gel form of DOPA modified polymers did not show any adhesion to the surfaces of SLPS when Fe^{3+} was being used as cross-linking agent. Both gel form of PEG-$(DOPA)_4$ and gel form of $(DOPA)_2$-PEG-$(Trp)_2$ did not adhere to the surfaces of the nanoparticles at pH=9.0. DOPA uses its two hydroxyl groups (-OH) for cross-linking. These groups are oxidized as the medium is basic. Fe^{3+} needs high pH values to make cross-linking with DOPA. In this medium, some of the DOPA can be oxidized to o-quinone. Therefore, they can not make bond with SLPS. However, IO_3^- ion based gel form of PEG-$(DOPA)_4$ adheres to the surface of SLPS. IO_3^- ion is a stronger oxidant than Fe^{3+} ion for cross-linking of DOPA. Also the gel is formed at pH is 3.0, and hydroxyl groups remain unoxidized. Therefore IO_3^- based gel form of PEG-$(DOPA)_4$ adhered to the surface of SLPS prominently.

All these results proved that DOPA could adhere to underwater surfaces without an external force. The more DOPA molecule is used, the stronger adhesion is achieved.

REFERENCES

Akdogan, Y.; Wei, W.; Huang, K.Y.; Kageyama, Y.; Danner, E.W.; Miller, D.R.; Rodriguez, N.R.M.; Waite, J.H.; Han, S. Intrinsic Surface-Drying Properties of Bioadhesive Proteins. *Angew. Chem.* 2014, 126, 11435 –11438

Huang, K.; Niu, Y.; Wang, L.; Liu, Y.; Chen, J.; Wang, R. pH-Induced Cross-Linking of Dopamine-Containing Block Copolymers with Fe3+ to Form Self-Healing Hydrogels. *Advanced Materials Research Vol.* 569 2012, 11-14.

Wei, W.; Yu, J.; Broomell, C.; Israelachvili, J.N.; Waite, J.H. Hydrophobic Enhancement of Dopa-Mediated Adhesion in a Mussel Foot Protein. *J. Am. Chem. Soc.* 2013, 135, 377−383. 11-14.

Zeng, X.; Westhaus, E.; Eberle, N.; Lee, B.; Messersmith, B.P. Synthesis and Characterization of DOPA-PEG Conjugates. *Polymer Preprints* 2000, 41(1), 989.

Krogsgaard, M.; Behrens, M.A.; Pedersen, J.S.; Birkedal, B. Self-Healing Mussel-Inspired Multi-pH-Responsive Hydrogels. *Biomacromolecules* 2013, 14, 297−301.

Lee, B.P.; Messersmith, P.B.; Israelachvili, J.N.; Waite, J.H. Mussel-Inspired Adhesives and Coatings. *Annu Rev Mater Res.* 2011, 1; 41: 99–132.

Dalsin, J.L.; Hu, B.H.; Lee, B.P.; Messersmith, P.B. Mussel Adhesive Protein Mimetic Polymers for the Preparation of Nonfouling Surfaces. *J. Am. Chem. Soc.* 2003, 125, 4253-4258

Akdogan, Y., Ph.D. Thesis. 2009, Institute of Physical Chemistry, Stuttgart University, Germany

Leng, C.;Liu, Y.; Jenkins, C.; Meredith, H.; Wilker, J.J.; Chen, Z. Interfacial Structure of a DOPA-Inspired Adhesive Polymer Studied by Sum Frequency Generation Vibrational Spectroscopy. *Langmuir* 2013, 29, 6659−6664 7882.

Westwood, G.; Horton, T.N.; Wilker, J.J. Simplified Polymer Mimics of Cross-Linking Adhesive Proteins. *Macromolecules* 2007, 40, 3960-3964.

Lin, Q.; Gourdon, D.; Sun, C.; Holten-Andersen, N.; Anderson, T.H.; Waite, J.H.; Israelachvili, J.N. Adhesion mechanisms of the mussel foot proteins mfp-1 and mfp-3. *PNAS* 2007, 104, 3782–3786.

Lee, B.P.; Dalsin, J.L.; Messersmith, P.B. Synthesis and Gelation of DOPA-Modified Poly(ethylene glycol) Hydrogels. *Biomacromolecules* 2002, 3, 1038-1047.

Mueller, C.; Capelle, M.A.H.; Arvinte, T.; Seyrek, E.; Borchard, G. Tryptophan-mPEGs: Novel excipients that stabilize salmon calcitonin against aggregation by non-covalent PEGylation. *European Journal of Pharmaceutics and Biopharmaceutics* 2011, 79, 646–657.

Mirshafian, R.; Wei, W.; Israelachvili, J.N.; Waite, J.H. α,β-Dehydro-Dopa: A Hidden Participant in Mussel Adhesion. *Biochemistry* 2016, 55, 743−750.

Giorgioni, G.; Claudi, F.; Ruggieri, S.; Ricciutelli, M.; Palmieri, G.F.; Di Stefano, A.; Sozio, P.; Cerasa, L.S.; Chiavaroli, A.; Ferrante, C.; Orlando, G.; Glennon, R.A. Design, synthesis, and preliminary pharmacological evaluation of new imidazolinon- es as L-DOPA prodrugs. *Bioorg. Med. Chem.* 18 (2010) 1834–1843

Belle, V.; Fournel, A.;Woudstra, M.; Ranaldi, S.; Prieri, F.; Thome´, V.; Currault, J.; Verger, R.; Guigliarelli, B.; Carrie`re, F., Probing the Opening of the Pancreatic Lipase Lid Using Site-Directed Spin Labeling and EPR Spectroscopy. *Biochemistry* 2007, 46, 2205-2214.

Sever, M.J.; Weisser, J.T.; Monahan, J.; Srinivasan, S.; Wilker, J.J, Metal-Mediated Cross-Linking in the Generation of a Marine-Mussel Adhesive. *Angew. Chem. Int. Ed.* 2004, 43, 447

APPENDIX

^{1}H-NMR SPECTRA OF COMPOUNDS

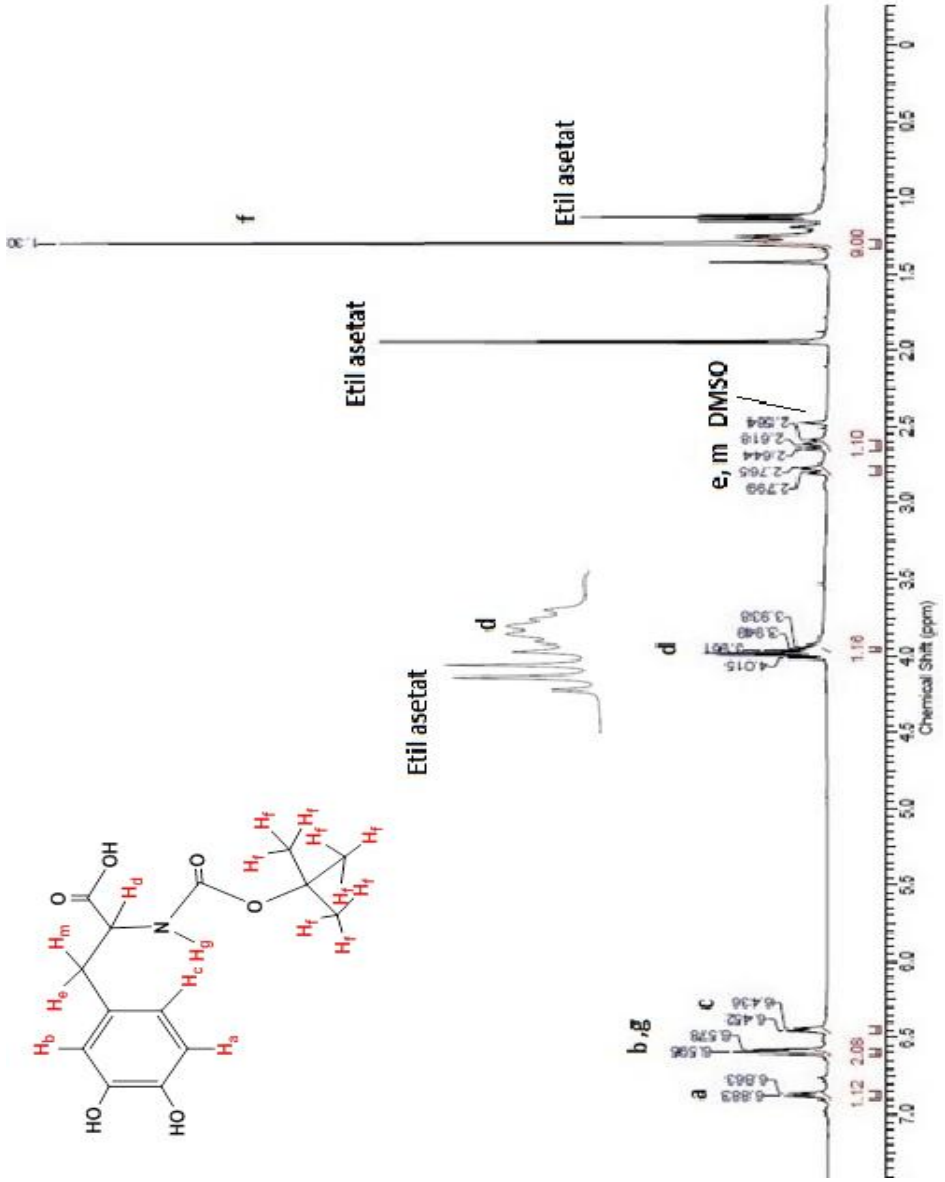

Figure A.1. ^{1}H NMR of N-Boc-L-DOPA molecule.

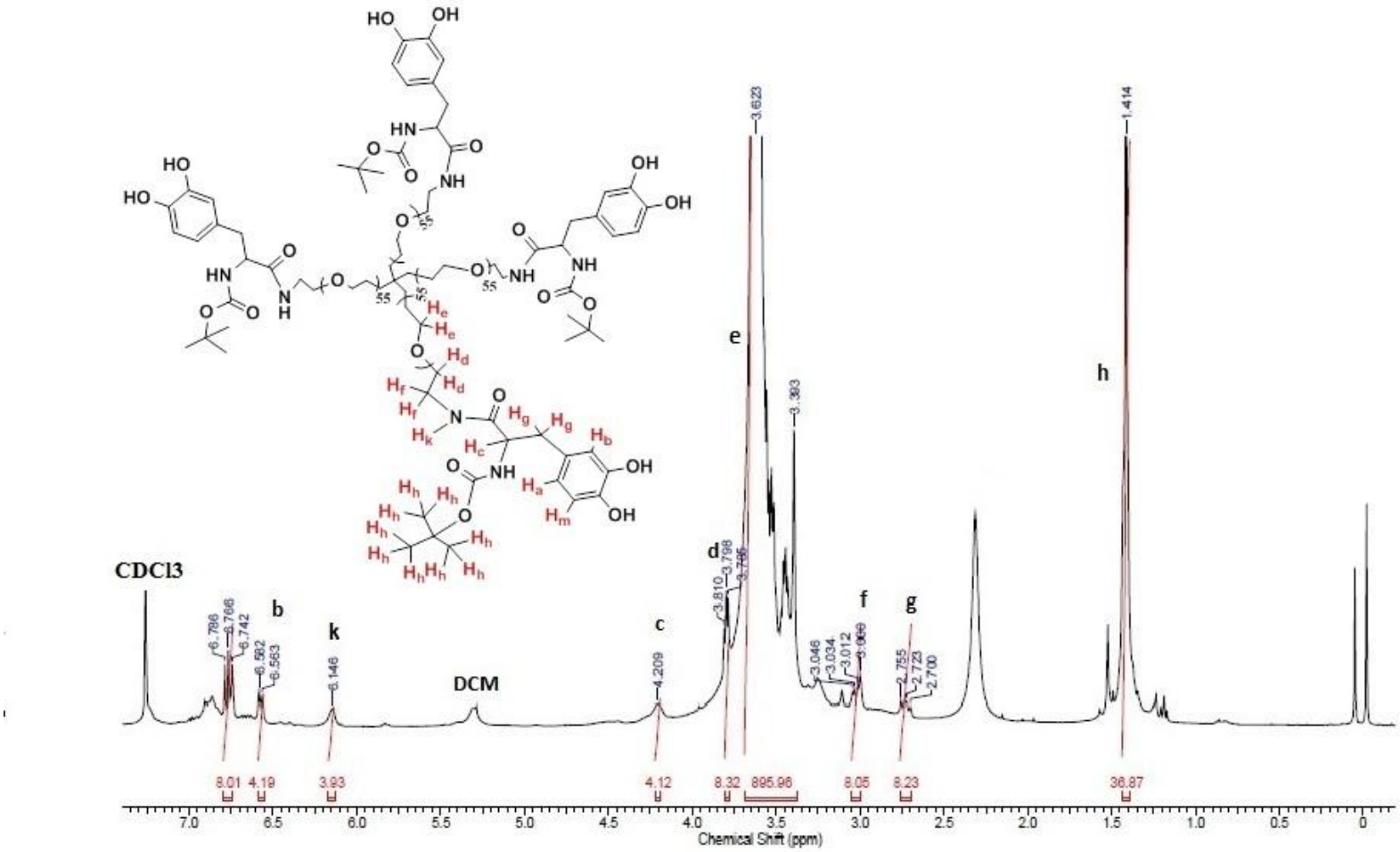

Figure A.2. ^{1}H NMR of PEG-(N-Boc-L-DOPA)$_4$ molecule.

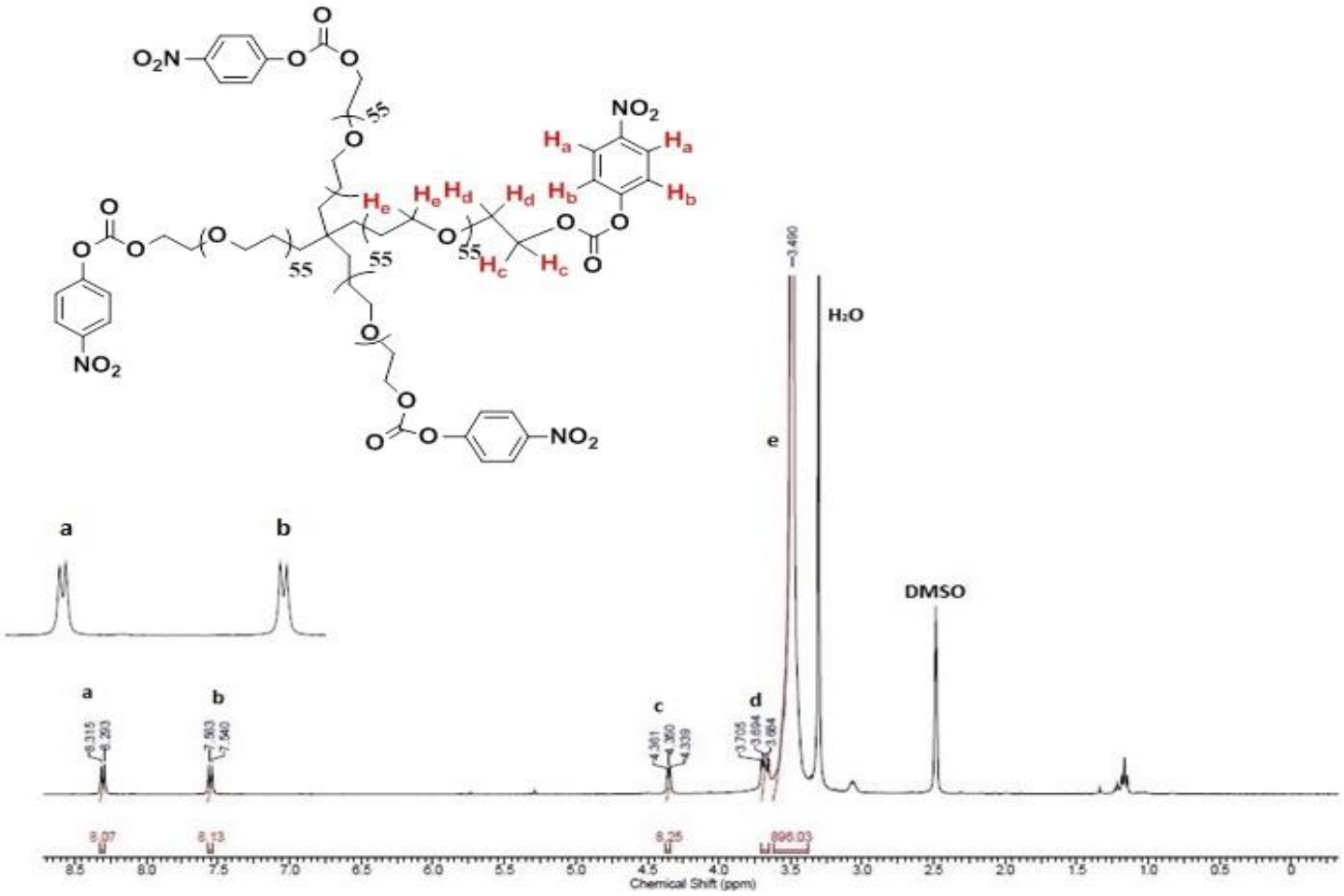

Figure A.3. ^{1}H NMR of PEG-(p-nitrophenylcarbonate)$_4$ molecule.

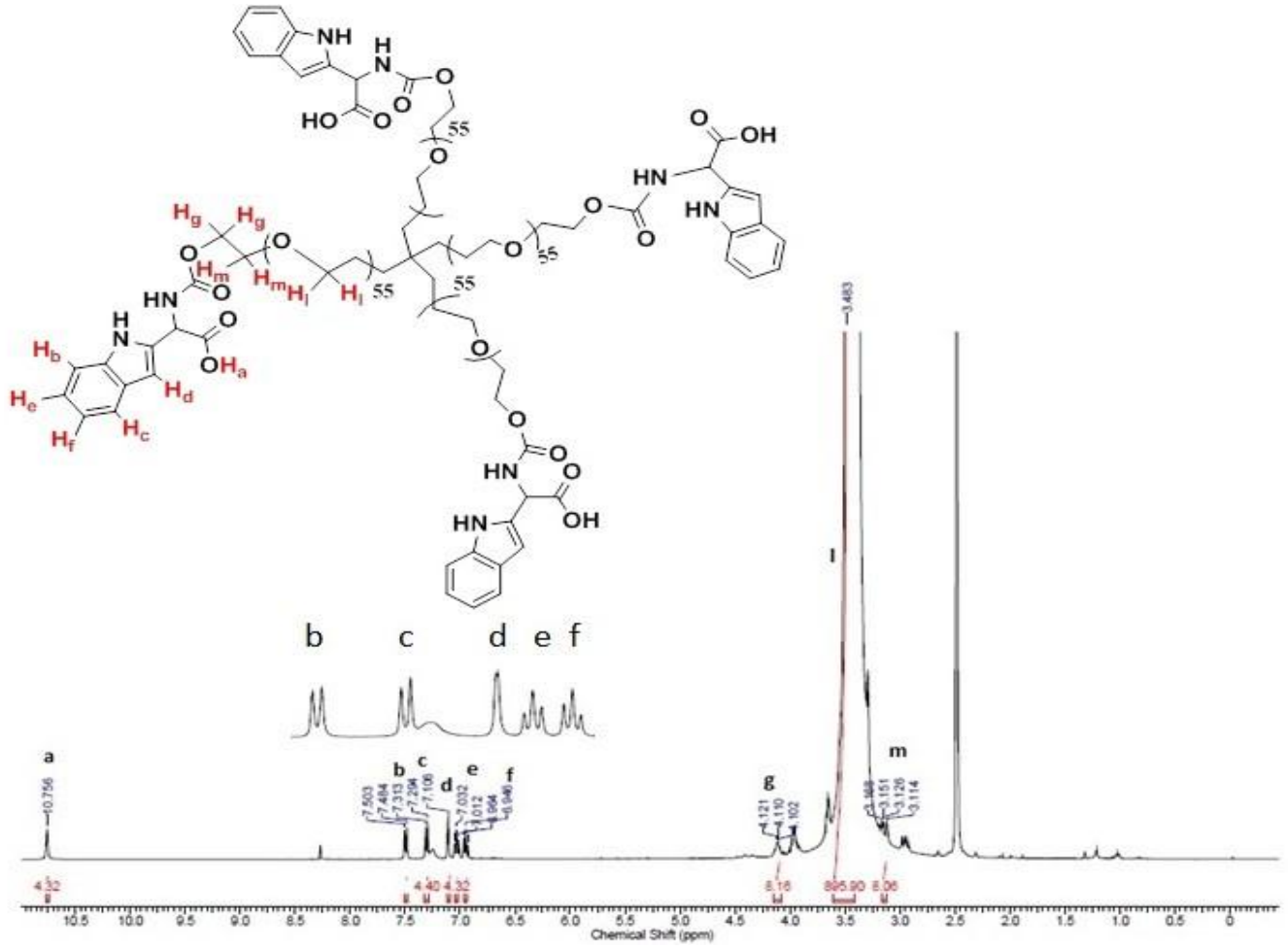

Figure A.4. ^{1}H NMR of PEG-$(Trp)_4$ molecule.

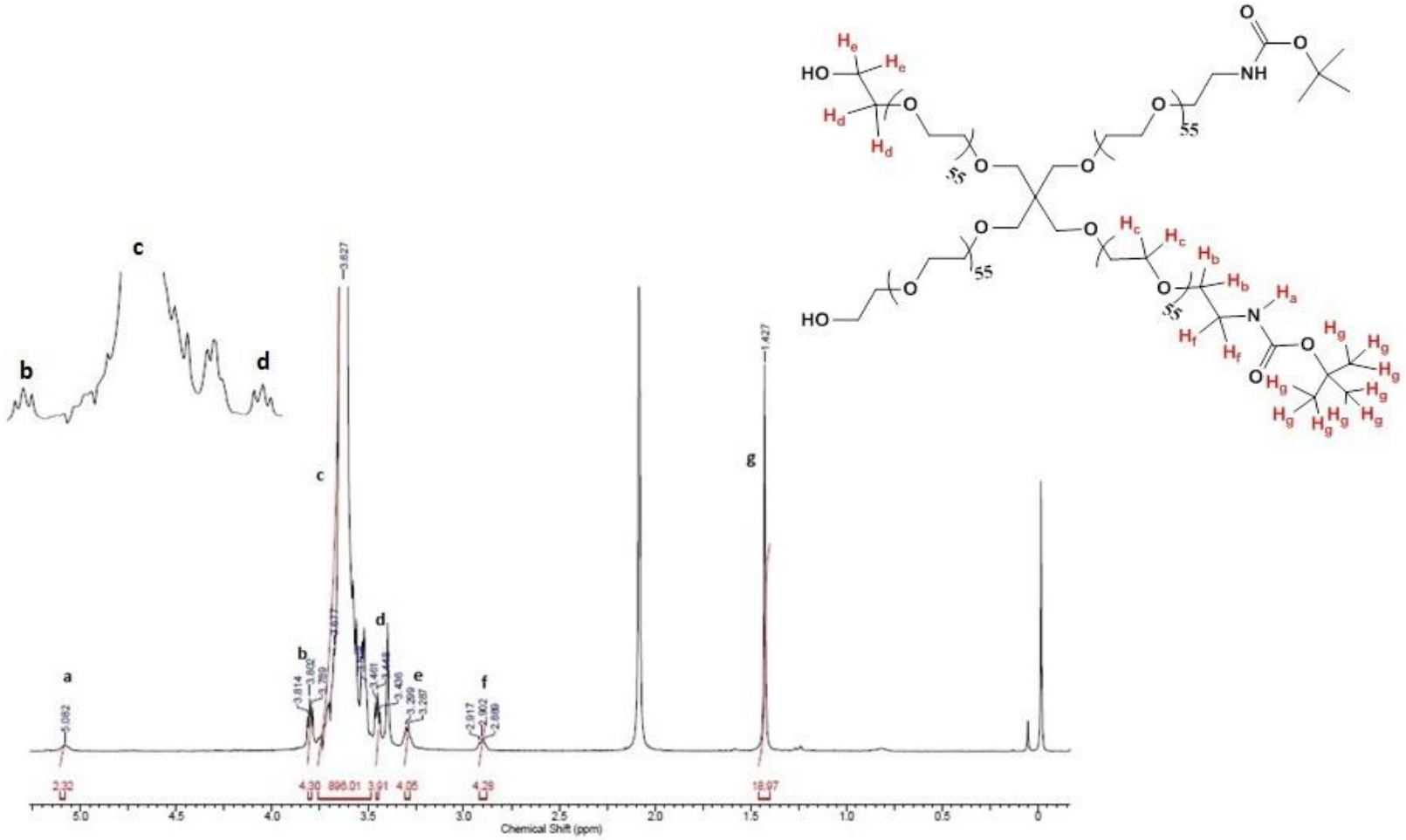

Figure A.5. ^{1}H NMR of $(N\text{-}Boc\text{-}H)_2\text{-}PEG\text{-}(OH)_2$ molecule.

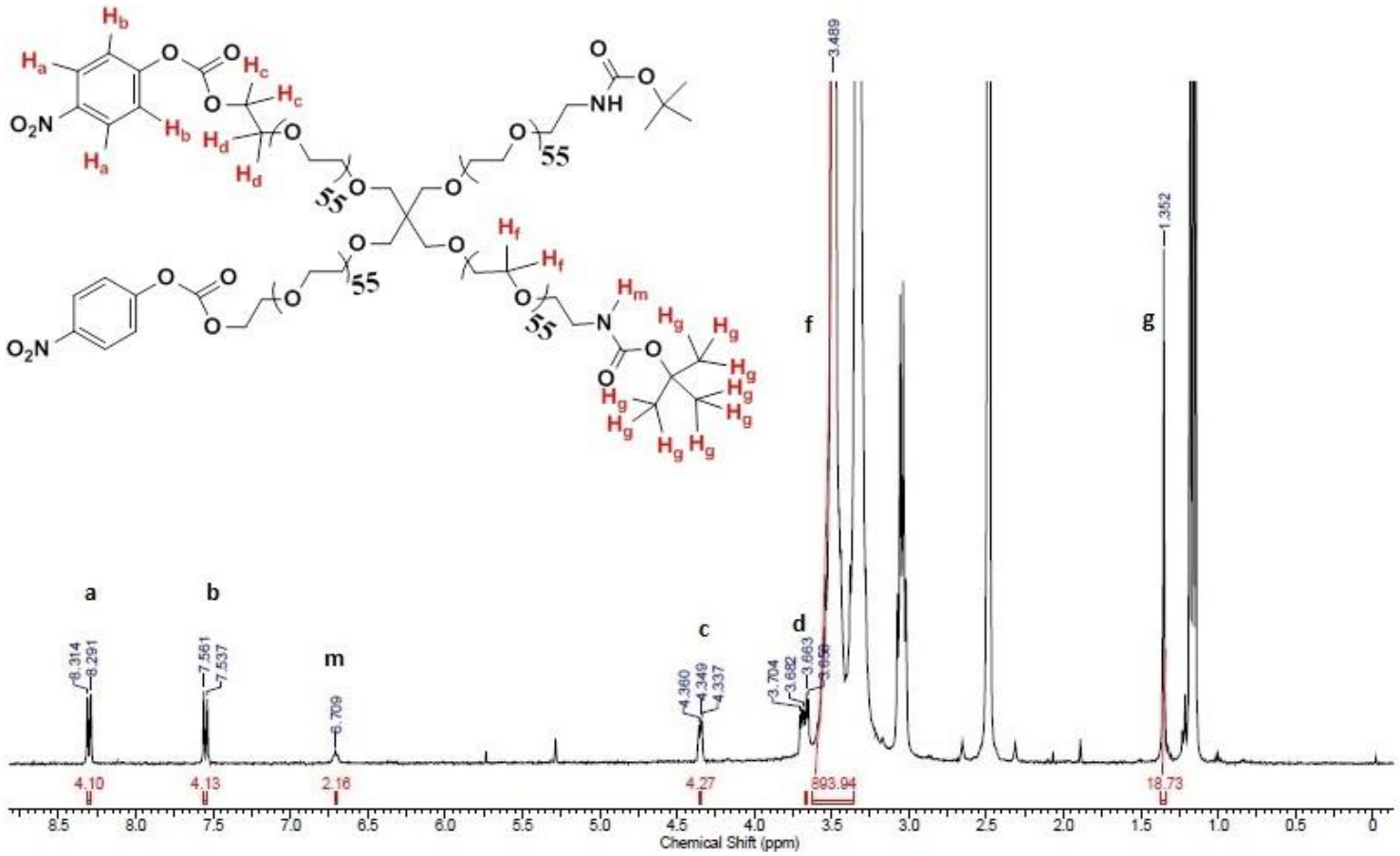

Figure A.6. ^{1}H NMR of (N-Boc-H)$_2$-PEG-(p-nitrophenylcarbonate)$_2$ molecule.

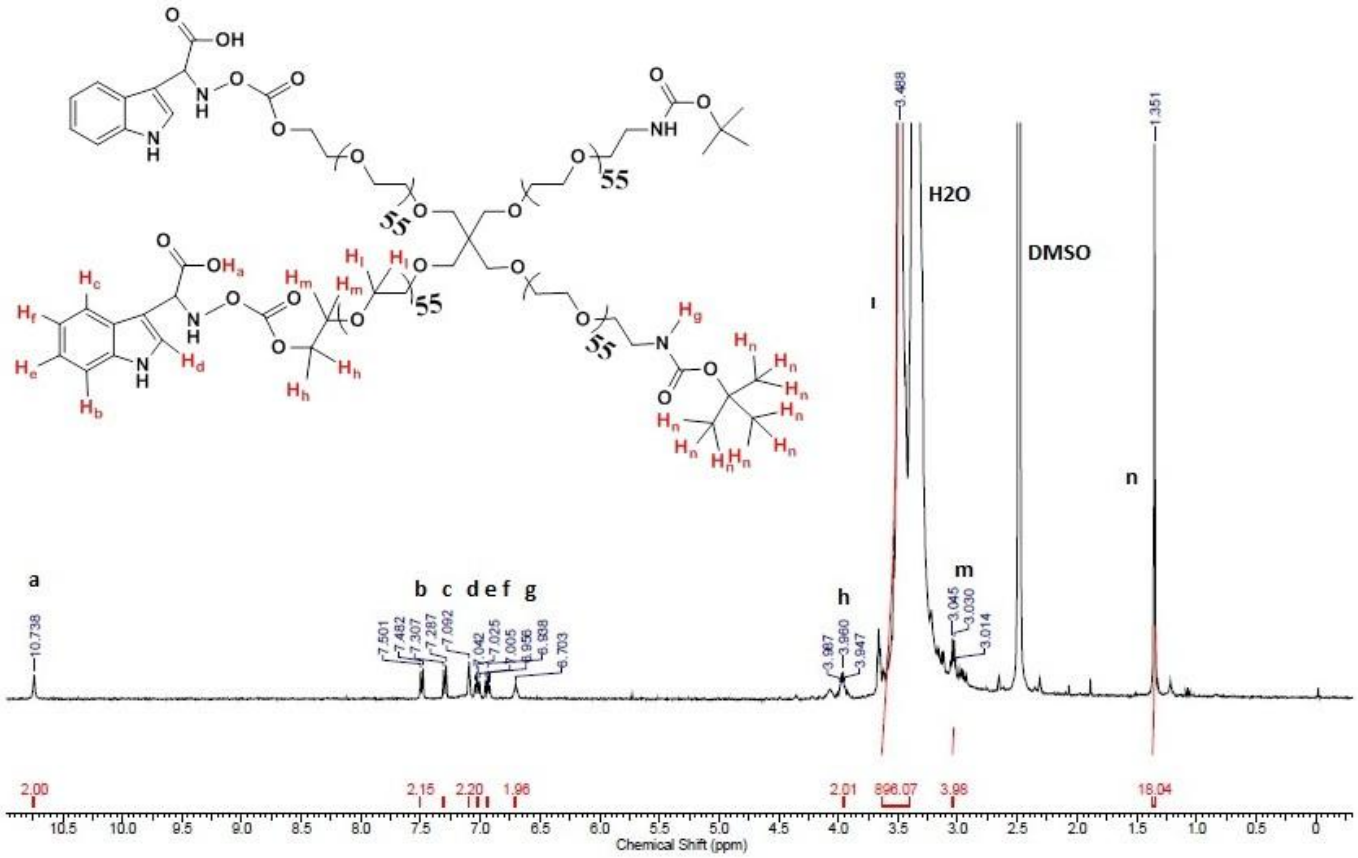

Figure A.7. ^{1}H NMR of $(N\text{-}Boc\text{-}H)_2\text{-}PEG\text{-}(Trp)_2$ molecule.

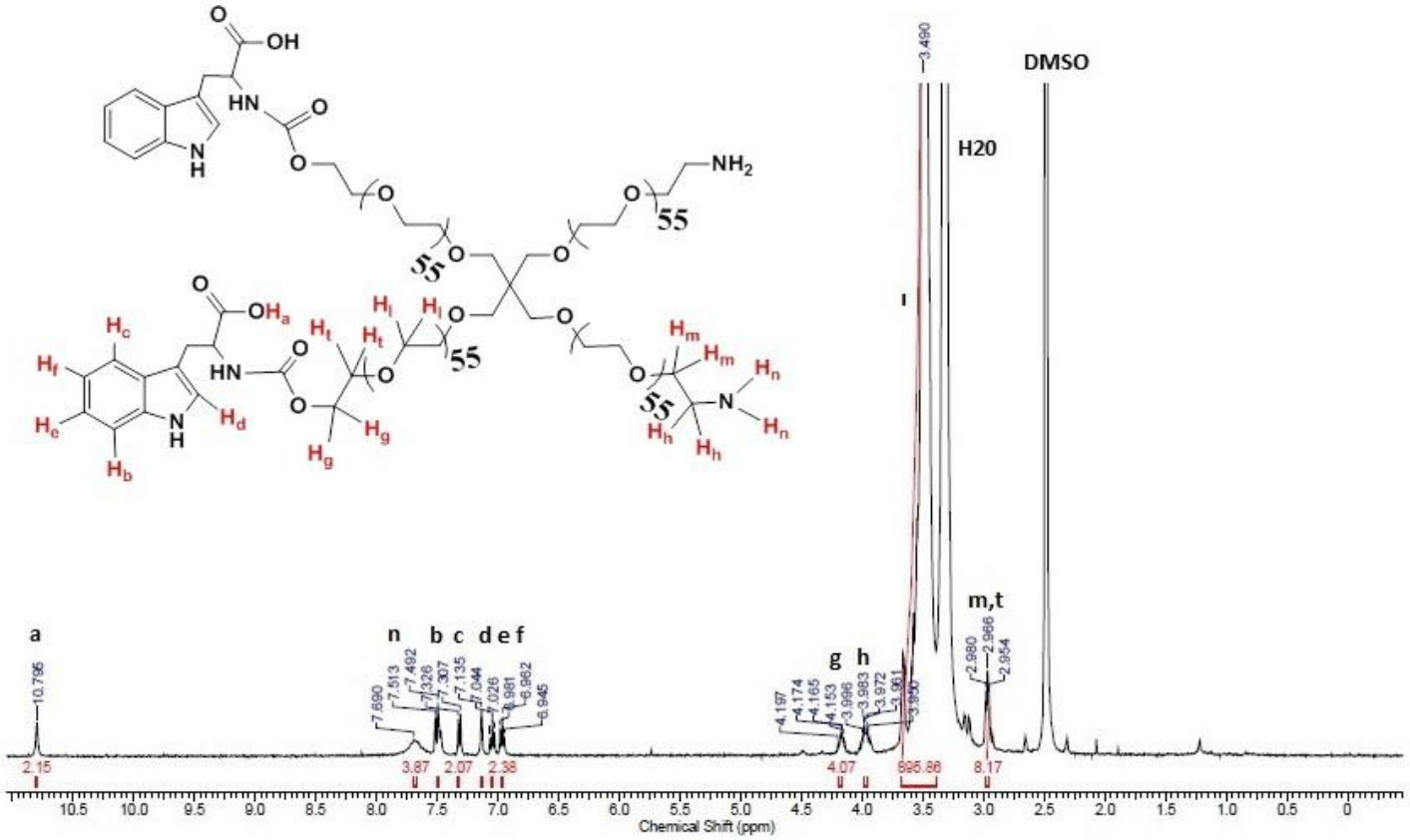

Figure A.8. ^{1}H NMR of $(NH_2)_2$-PEG-$(Trp)_2$ molecule.

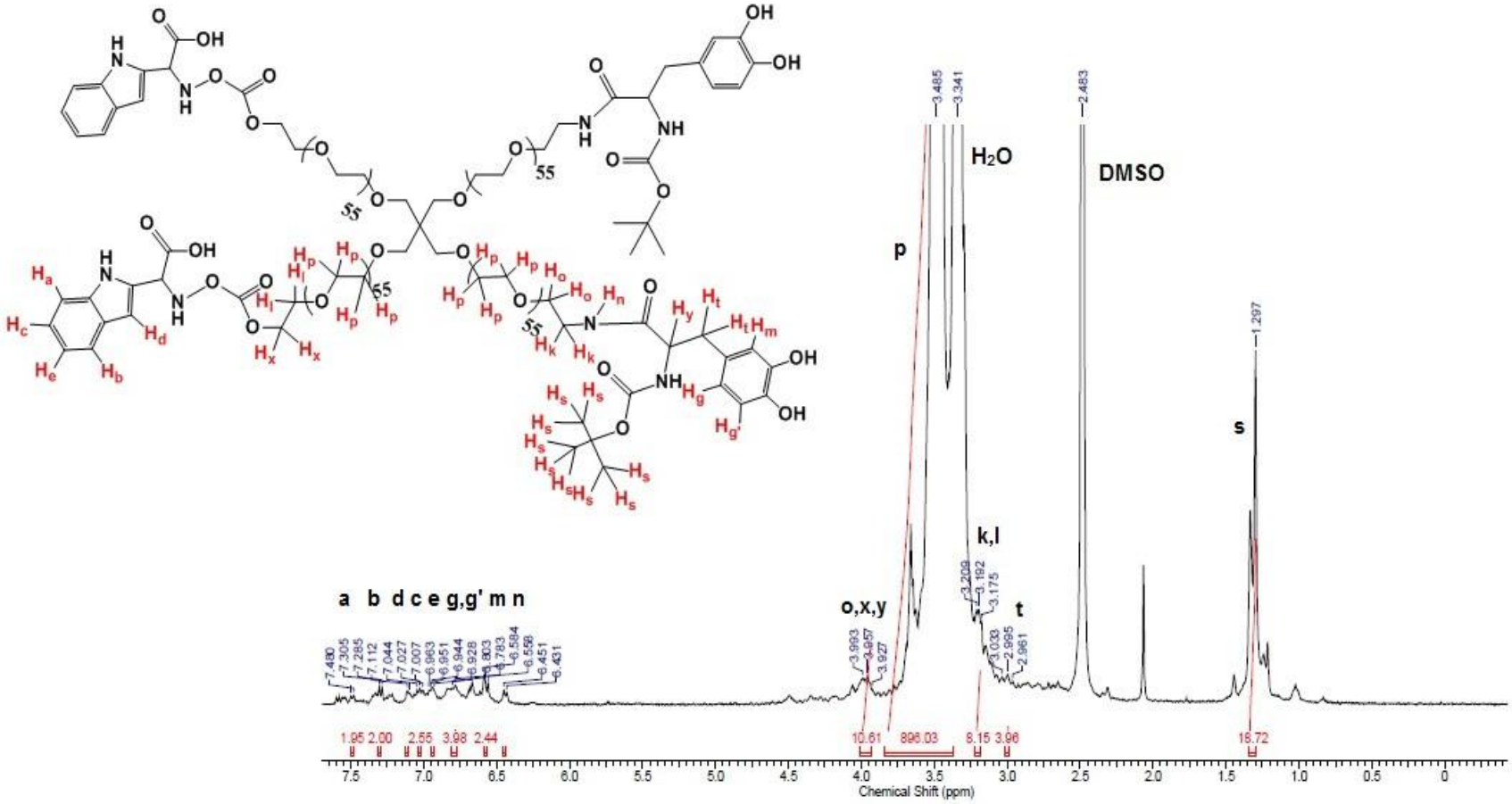

Figure A.9. ^{1}H NMR of (N-Boc-L-DOPA)$_2$-PEG-(Trp)$_2$ molecule.